

# **U-Pb zircon geochronology results for Ujarassuit Nunaat supracrustal belts and surrounding gneisses**

Interim report

Julie A. Hollis, Nigel M. Kelly, Dirk Frei, Susanne Schmid  
& Jeroen A. M. van Gool



GEOLOGICAL SURVEY OF DENMARK AND GREENLAND  
MINISTRY OF THE ENVIRONMENT

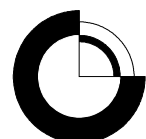


**G E U S**

# **U-Pb zircon geochronology results for Ujarassuit Nunaat supracrustal belts and surrounding gneisses**

Interim report

Julie A. Hollis, Nigel M. Kelly, Dirk Frei, Susanne Schmid  
& Jeroen A. M. van Gool



## Summary

This interim report comprises new zircon U-Pb geochronology data for rock samples collected during a 2005 mapping campaign on Ujarassuit Nunaat in the Nuuk region, southern West Greenland. Zircons separated from the samples were analysed for U-Pb isotopes using the GEUS in-house laser ablation-sector field-inductively coupled plasma-mass spectrometer facility. The findings shed new light on the timing of formation and metamorphism of supracrustal belts in this area, and on the regional orthogneisses.

Mesoarchaean (or older) orthogneisses exist throughout the Ujarassuit area. The amphibolitic supracrustal belt in Ujarassuit area 8 is intruded by c. 3010 Ma leucogranitic gneiss. Likewise, supracrustal rocks in Ujarassuit area 6 are intruded by a  $\geq$  3025 Ma tonalitic leucogneiss. These supracrustal belts were therefore deposited prior to those times. A relatively old magmatic component of a biotite-felsic orthogneiss from area 4 was emplaced at  $\geq$  2974 Ma (sample 498864), confirming data of C.R.L. Friend (pers. comm.) and furthering the extent of (probable) Mesoarchaean orthogneisses in the Ujarassuit area.

Three samples of weakly deformed felsic orthogneisses from Ujarassuit area 9 (sample 498420), area 6 (sample 498496), and area 4 (sample 498877) represent relatively young phases of magmatism. Emplacement is constrained to c. 2870 Ma,  $\geq$  2750 Ma and  $\geq$  c. 2825 Ma respectively. They are deformed by 10 kilometre-scale folds (Hollis et al. 2006).

A biotite orthogneiss representative of gneisses from within Ujarassuit area 5 yielded evidence for an emplacement age of  $\geq$  c. 3373 Ma, where these rocks were previously mapped as Nûk gneiss (c. 3070 Ma). Results from more structurally complex gneisses further east, across a mapped lithological boundary, confirmed a previous interpretation that those are Eoarchaean gneisses ( $3872 \pm 43$  Ma; Chadwick and Coe 1988).

Intermediate composition amphibolites of inferred volcanic origin from Ujarassuit area 4 (sample 498892) and area 5 (sample 498945) yielded evidence for deposition probably at around 3400 Ma. These are the first recorded supracrustal rocks of this age in the Nuuk region and further work should be done to investigate their timing of formation and regional significance. The same rocks from area 5 (sample 498945) contain metamorphic zircon dated at  $3056 \pm 5$  Ma, possibly related to the emplacement of Nûk gneisses at this time.

Samples from within the supracrustal belts in area 9 (sample 498422), area 8 (sample 498447), and area 1 (sample 498803) yielded metamorphic zircon dated at  $2598 \pm 10$  Ma,  $2617 \pm 6$  Ma,  $2609 \pm 14$  Ma respectively. These indicate that a Neoarchaean metamorphic event affected a large part of the Ujarassuit area. Similar metamorphic ages (and also up to c. 2700 Ma) were previously established for samples from Storø (Hollis 2005) – a c. 2700 Ma amphibolite facies event is known to have affected most of the Nuuk region (Nutman et al. 1989, Friend et al. 1996).

Results from central Storø show that the felsic orthogneiss structurally underlying the supracrustal belt on central Storø (sample 496516) is Mesoarchaean, emplaced at c. 3050 Ma. This is consistent with data from Hollis (2005) for a tonalitic gneiss intrusive into the metagabbro-anorthosite that lies structurally beneath the supracrustal belt on Storø.

# Introduction

The U-Pb zircon geochronology data presented here were obtained in 2006 for samples collected during a 2005 mapping campaign in the Ujarassuit area (see Hollis et al. 2006). The mapping was carried out by Ali Polat and Carlos Ordóñez (University of Windsor), Nigel Kelly (University of Edinburgh), Ole Stecher, Jeroen van Gool, and Susanne Schmid (GEUS). This mapping work forms part of an ongoing GEUS program to understand the geological setting of formation and tectonothermal evolution of supracrustal rocks in the Nuuk region, southern West Greenland (see also Appel et al. 2003, Hollis et al. 2004, Hollis 2005, Hollis et al. 2006, Nielsen et al. 2004, Stensgaard et al. 2005). A summary of the regional geology is given in Appel et al. (2003) and Hollis et al. (2004).

The complete tabulated data are presented in Appendix 1. Each analysed sample is discussed in the text and relevant data is presented in age plots. The areas mapped (areas 1–9), referred to in the text in relation to sample locations, are shown in Figure 1. The sample localities along with summary age information are shown in Figs 2–7 and in Table 1.

**Table 1.** Geochronology samples. Main abbreviations: *D* – depositional age, *E* – emplacement age, *heterog* – heterogeneous, *homog* – homogeneous, *M* – metamorphic age

Sample	Latitude	Longitude	UTM N	UTM E	Area	Description	Aim	Age
496513	64 27.812°	-50 55.612	7148667	503518	Storø	felsic sheet cutting felsic orthogneiss structurally underlying supracrustal belt, central Storø	min age of gneissosity in felsic orthogneiss structurally underlying supracrustals, Storø	E: c. 2715 Ma? or 2981 Ma?
496516	64 27.397	-50 58.346	7147894	501325	Storø	felsic orthogneiss structurally underlying anorthosite, central Storø	E age of orthogneiss structurally underlying supracrustal belt, central Storø	E: 3045 ± 13 Ma
496519	64 18.289	-51 20.243	7131022	483677	Sermitsiaq	deformed aplitic sheet post-dating start of cataclasis in shear zone, Sermitsiaq	min age of onset of cataclasis	E: ? ≤ c. 2850 Ma M: c. 2670 Ma
498420	64 53.202	-50 14.203	7196046	536146	9	bi-bearing TTG gneiss	age of youngest magmatic phase, max constraint on formation of regional F3	E: ≤ c. 2870 Ma
498422	64 53.353	-50 13.699	7196330	536540	9	homog hbl gneiss, originally gabbro?, forms a part of mafic amphibolite sequence, or is a later intrusion	age of youngest magmatic phase, max constraint on formation of regional F3	M: 2598 ± 10 Ma
498447	64 57.044	-50 17.446	7203151	533506	8	homog hbl-bearing qtz-dioritic gneiss that forms an integral part of the supracrustal unit	age of formation of part of area 8 supracrustal belt	M: 2617 ± 6 Ma
498452	64 57.082	-50 17.616	7203222	533371	8	leucogranite intruded into amphibolitic supracrustals	min age of supracrustal belt, min age of gneissosity in supracrustals	E: > c. 3010 Ma
498481	64 58.741	-50 25.764	7206237	526928	6	late aplitic dyke cutting Tasersuaq pluton	min age of deformation of the Tasersuaq pluton	E: ?2936 ± 13 Ma
498496	64 58.193	-50 23.122	7205240	529016	6	deformed homog tonalitic bi orthogneiss, discordant to older gneissosity	timing of relatively young magmatism	E: ≥ 2750 Ma
498497	64 58.184	-50 23.765	7205218	528510	6	deformed pegmatite postdates main gneissosity in orthogneiss and deformed by shear-fabric	min age of formation of regional gneissosity, max constraint on later deformation	E: ≥ c. 2645 Ma

**Table 2 continued.** Geochronology samples. Main abbreviations: *D* – depositional age, *E* – emplacement age, *heterog* – heterogeneous, *homog* – homogeneous, *M* – metamorphic age.

Sample	Latitude	Longitude	UTM N	UTM E	Area	Description	Aim	Age
498762	64 58.544	-50 24.344	7205881	528048	6	homog tonalitic leucogneiss intrusive into supracrustal rocks, and representative of the dominant felsic orthogneisses	emplacement age of dominant regional orthogneiss in area 6	E: $\geq$ 3025 Ma
		.						
498803	64 50.622	-50 12.786	7191268	537320	1	migmatitic grt-bi schist, inferred sedimentary or volcanic origin	age of deposition	M: $2609 \pm 14$ Ma
498864	64 48.696	-50 24.414	7187592	528162	4	heterog migmatitic bi-felsic orthogneiss. Older phase of magmatism	age of early phase of magmatism	E $\geq$ 2974 Ma
498877	64 49.638	-50 24.744	7189346	527884	4	massive felsic bi orthogneiss. Youngest phase of magmatism, post-dating main gneissosity	age of youngest phase of magmatism	E: $\geq$ c. 2825 Ma
498892	64 48.396	-50 24.912	7187036	527776	4	intermediate amphibolite, inferred volcanic origin	volcanic depositional age	D: ? c. 3400 Ma
498921	64 45.918	-50 32.310	7182382	521949	5	felsic-intermediate bi orthogneiss	emplacement of dominant felsic orthogneiss	E: $\geq$ c. 3373 Ma
498937	64 46.008	-50 29.664	7182563	524046	5	felsic bi orthogneiss	emplacement of dominant felsic orthogneiss	E: $3872 \pm 43$ Ma
498945	64 46.662	-50 30.720	7183769	523202	5	garnet-bearing amphibolite, inferred volcanic origin	volcanic deposition	D: c. 3400 Ma M: $3056 \pm 5$ Ma
		.						

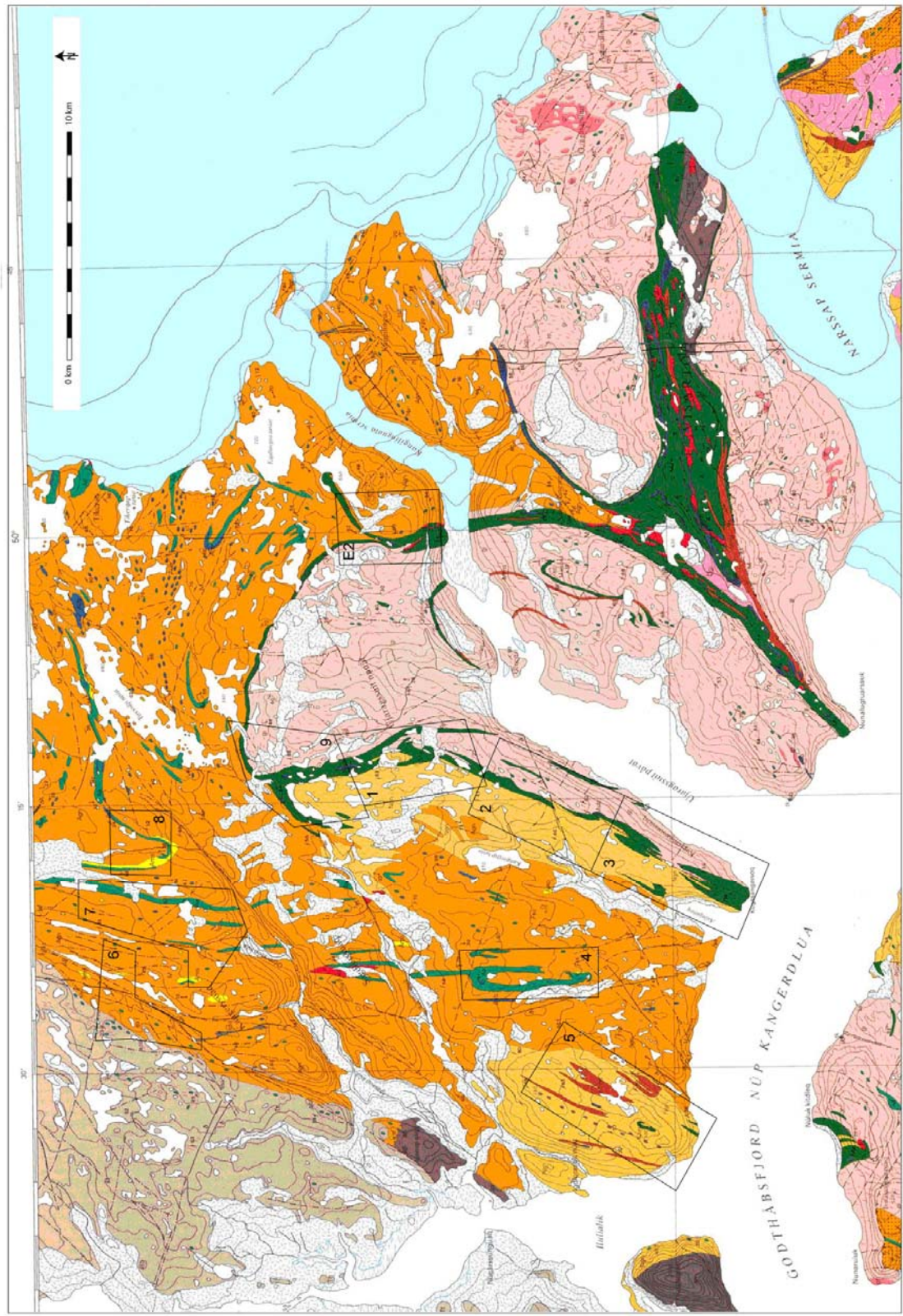


**Figure 1.** Mapped areas referred to the in the text, labelled 1 to 9.

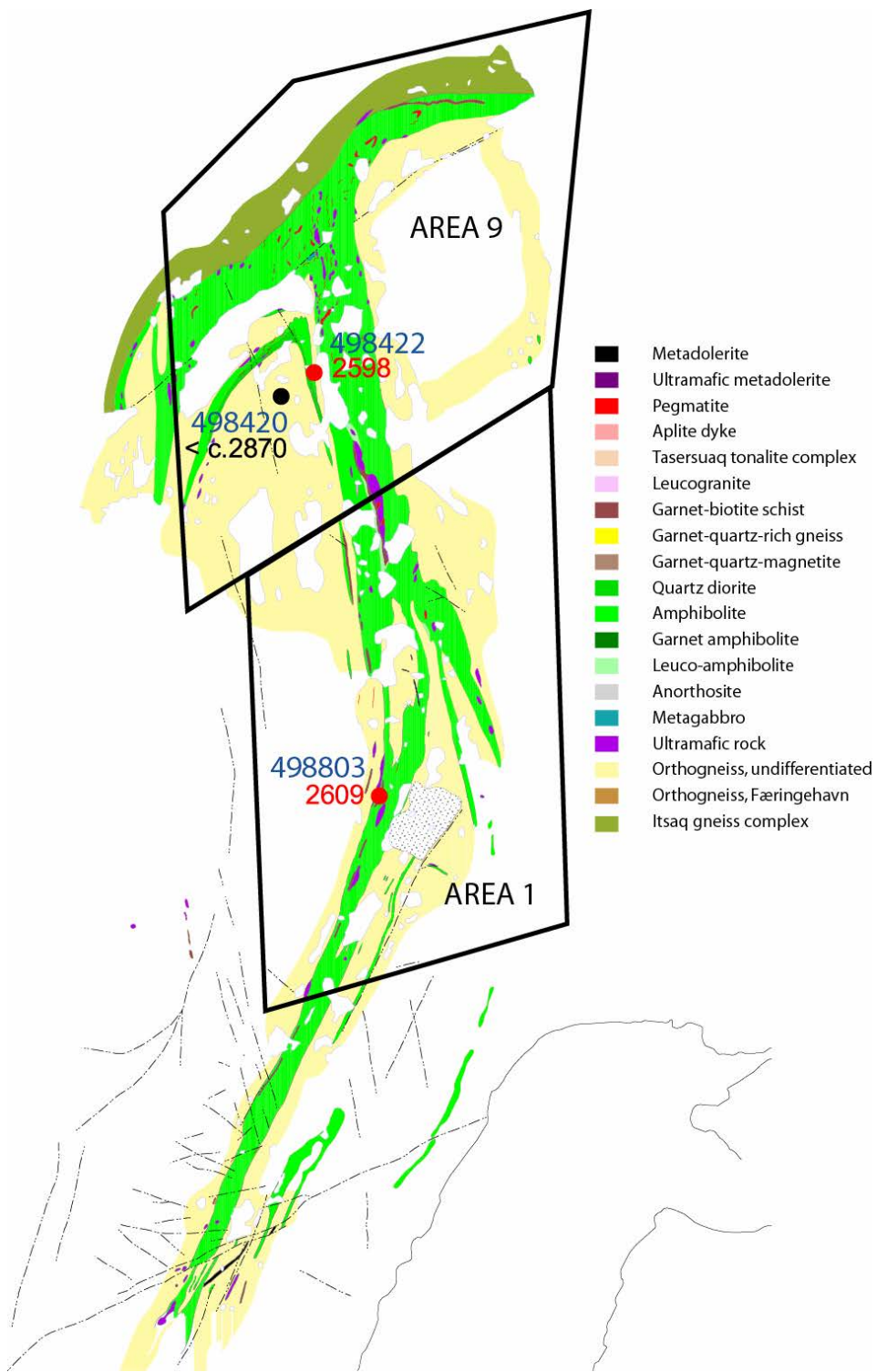


**Figure 2.** Geological map of areas 1 and 9 (from Hollis et al. 2006) showing sample localities, sample numbers, and summary ages. Emplacement ages are shown in black and metamorphic ages in red. For regional context see Figure 1.

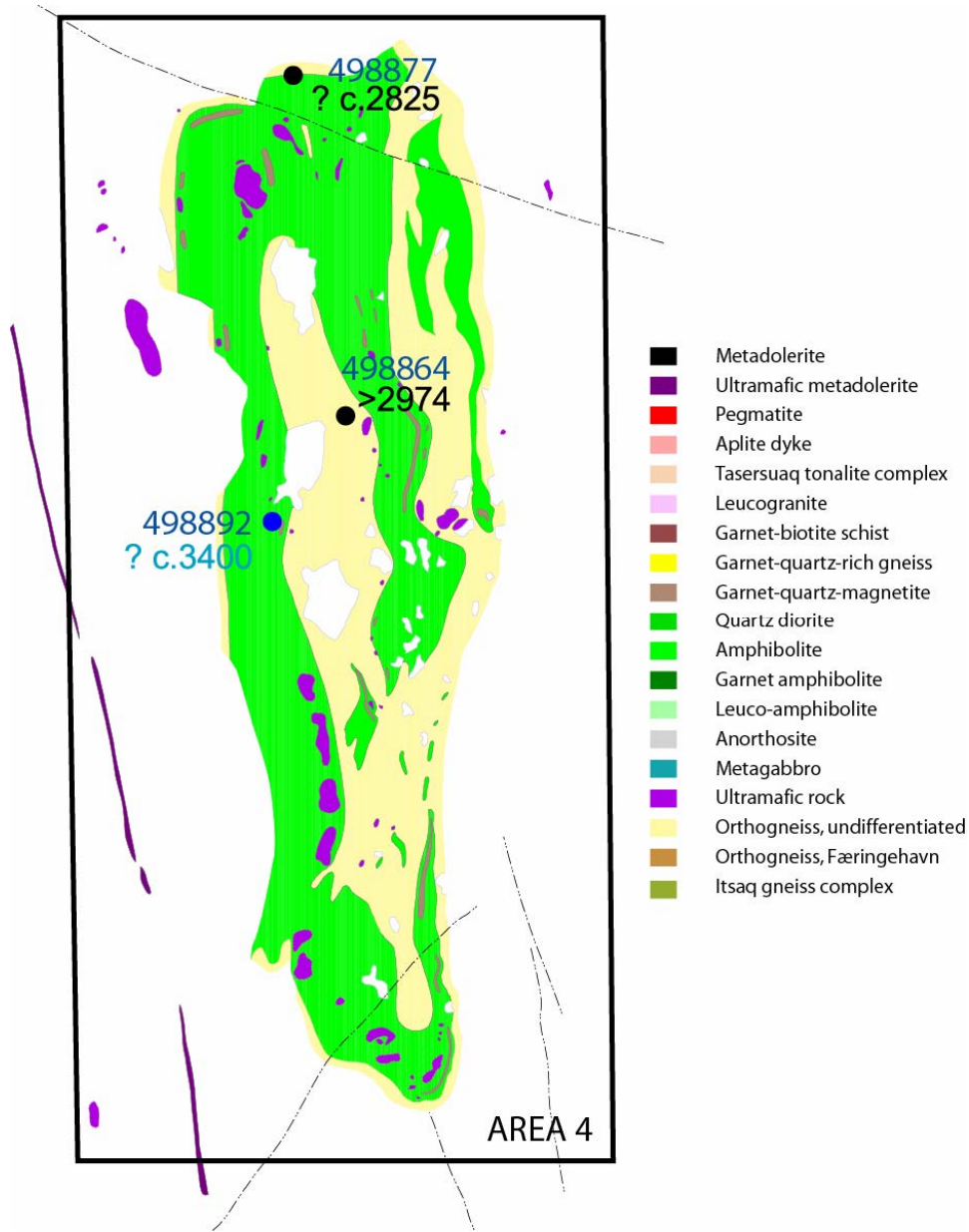


**Figure 3.** Geological map of area 4 (from Hollis et al. 2006) showing sample localities, sample numbers, and summary ages. Emplacement ages are shown in black and depositional ages in blue. For regional context see Figure 1.

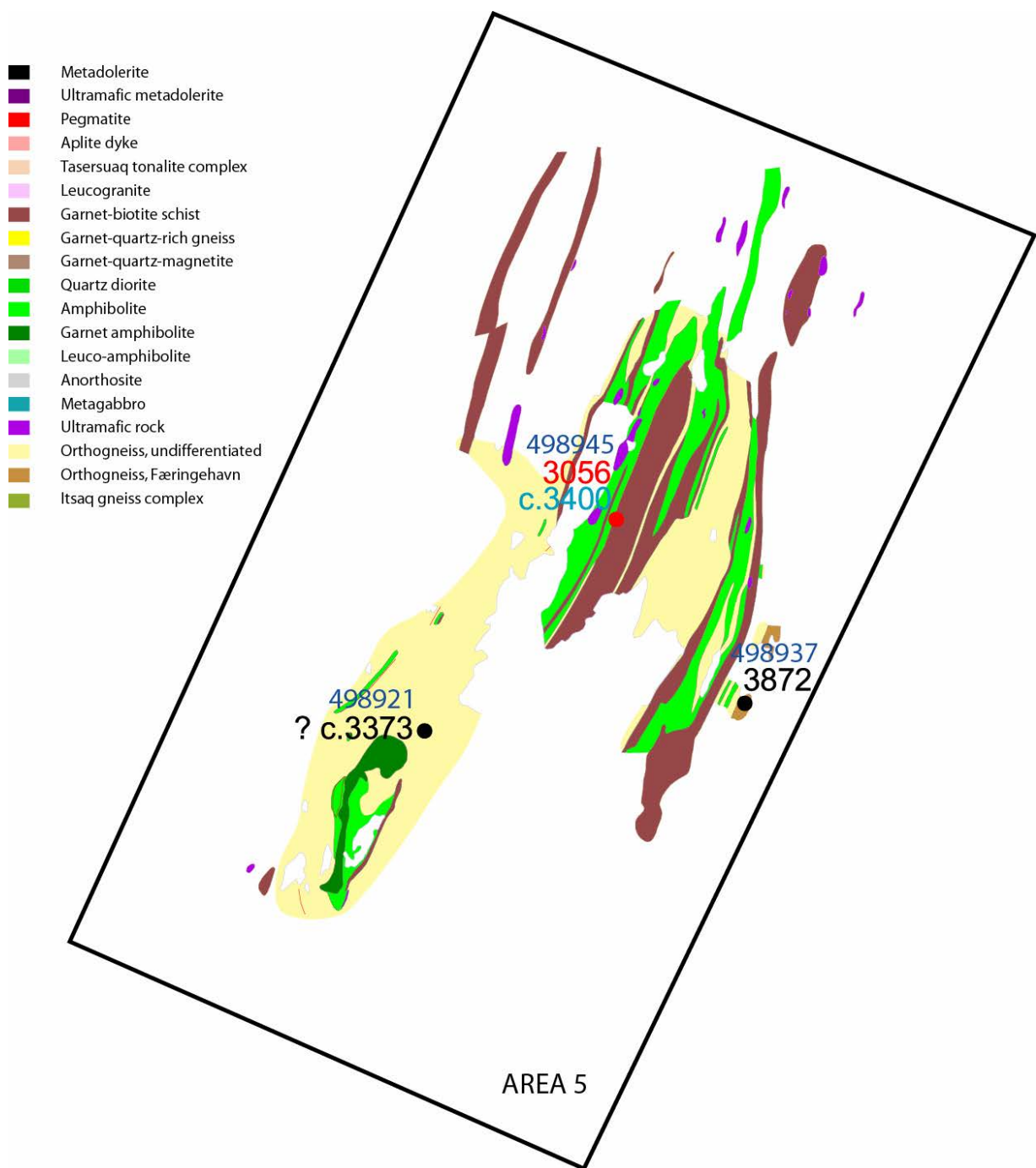


**Figure 4.** Geological map of area 5 (from Hollis et al. 2006) showing sample localities, sample numbers, and summary ages. Emplacement ages are shown in black, depositional ages are shown in blue, and metamorphic ages in red. For regional context see Figure 1.

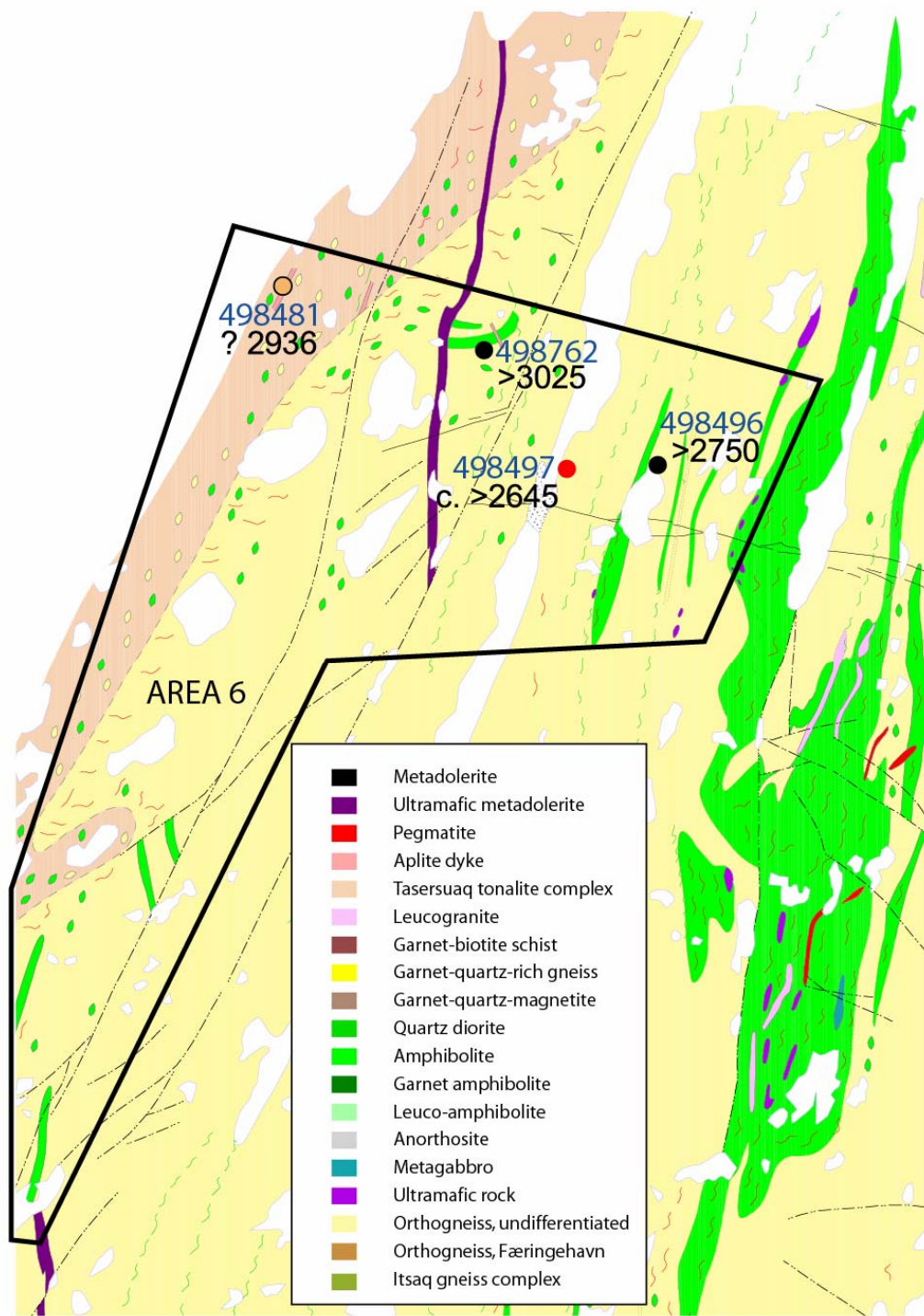


**Figure 5.** Geological map of area 6 (from Hollis et al. 2006) showing sample localities, sample numbers, and summary ages. Emplacement ages are shown in black. For regional context see Figure 1.

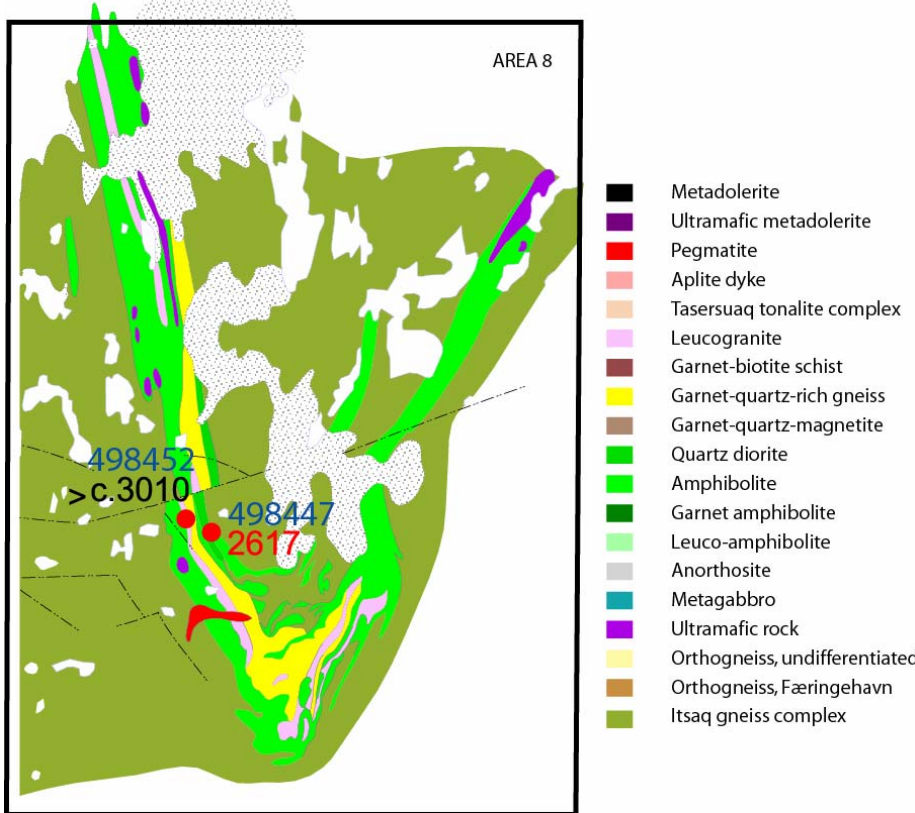


**Figure 6.** Geological map of area 8 (from Hollis et al. 2006) showing sample localities, sample numbers, and summary ages. Emplacement ages are shown in black and metamorphic ages in red. For regional context see Figure 1.

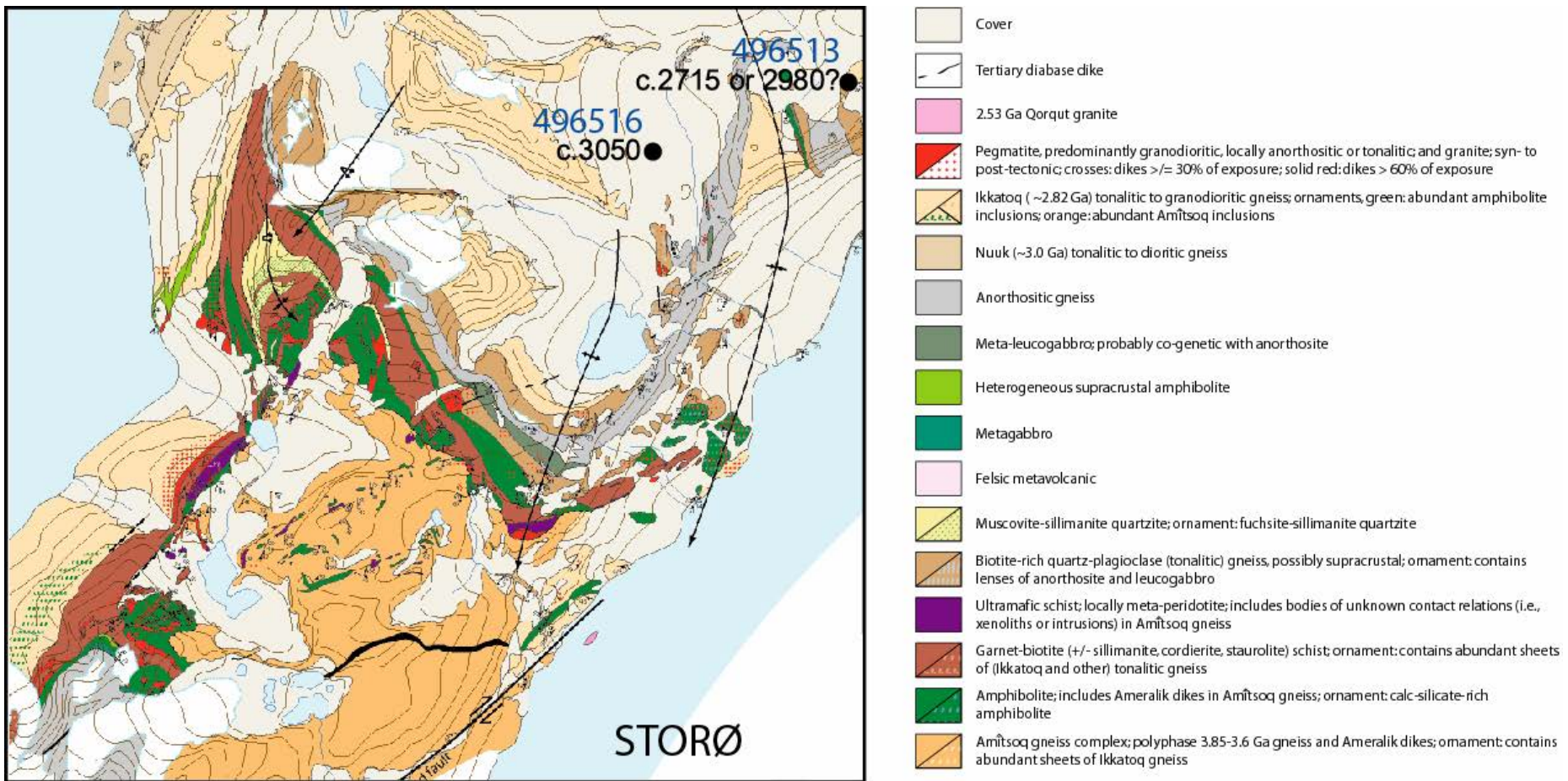


**Figure 7.** Geological map of central Storø showing sample localities, sample numbers, and summary ages. Emplacement ages are shown in black.

# Geochronology

## Sample preparation

Rock samples were typically hammered into small, centimetre- to decimetre-scale fragments on the outcrop. This was done to avoid potential contamination by breaking up the sample in the laboratory. Remaining large samples were sawed into small pieces, crushed to a coarse powder in a steel ring mill, and sieved to obtain the  $< 400 \mu\text{m}$  fraction. Powders were separated by hand-panning and the heavy-fraction was further separated where required using a magnet. The non-magnetic heavy fraction obtained typically included phases such as zircon, titanite, rutile, and sulphide minerals.

Individual zircon grains were hand-picked from the heavy mineral fraction under an optical binocular microscope. These were mounted in rows on double-sided sticky tape. The mounted zircons were then set in one inch diameter circular epoxy mounts, which were then ground to reveal the mid-sections of the zircon grains, and polished to one micron grade.

The polished zircons were imaged using cathodoluminescence (CL) or back-scattered electron (BSE) imaging employing a Philips XL 40 scanning electron microscope at GEUS. Images were used to identify the internal morphology of grains (influenced by, for example, growth, resorption, alteration, or metamorphism) to select areas of interest for analysis.

## Laser ablation – inductively coupled plasma – sector field mass spectrometry (LA-SF-ICPMS) methodology

The LA-SF-ICPMS uses a focussed laser beam to ablate a small amount of a sample contained in an air-tight sample cell. The ablated material is transferred to a mass-spectrometer in a carrier gas via tygon tubing for isotopic quantification. For the spot diameter ( $30 \mu\text{m}$ ) and ablation times (45 s) used in this study, the ablated masses of zircon were approximately 200–500 ng.

The laser ablation system used at GEUS was a NewWave Research/Merchantek UP213 equipped with a frequency quintupled Nd-YAG laser emitting at a wavelength of 213 nm. The nominal pulse width of the laser is 5 ns with a pulse-to-pulse stability of 2 % RSD. The laser was operated at a repetition rate of 10 Hz and a nominal energy output of 44 %, corresponding to a laser fluency of  $8 \text{ J cm}^{-2}$ . All data were acquired with a single spot analysis on each individual zircon grain with a beam diameter of  $30 \mu\text{m}$  producing a spot with depth of c.  $15 \mu\text{m}$ . Samples and standards were held in a low-volume ablation cell designed in order to achieve fast flush-out times and stable, spike-free, time-resolved signals. He was used to flush the sample cell and was mixed downstream with the Ar sample gas of the

mass-spectrometer. The washout time for this configuration was approximately 20 s. All sample mounts were rigorously cleaned before introduction into the sample cell to remove surface Pb contamination.

The ablated material was analysed with an Element2 (ThermoFinnigan, Bremen) single-collector double focusing magnetic sector ICPMS equipped with a fast field regulator for increased scanning speed. The total acquisition time for each analysis was 100 s with the first 30 s used to measure the gas blank. The instrument was tuned to give large, stable signals for the  $^{206}\text{Pb}$  and  $^{238}\text{U}$  peaks, low background count rates (typically around 300 counts per second for  $^{207}\text{Pb}$ ) and low oxide production rates ( $^{238}\text{U}^{16}\text{O}/^{238}\text{U}$  generally below 2 %). All measurements were performed in low resolution mode using electrostatic scanning (E-scan) with the magnetic field resting at mass  $^{202}\text{Hg}$ . The following masses were measured:  $^{202}\text{Hg}$ ,  $^{204}(\text{Pb} + \text{Hg})$ ,  $^{206}\text{Pb}$ ,  $^{207}\text{Pb}$ ,  $^{208}\text{Pb}$ ,  $^{232}\text{Th}$ ,  $^{235}\text{U}$ , and  $^{238}\text{U}$ . All data were acquired on four samples per peak with a sampling time of 10 ms for most isotopes (except  $^{204}(\text{Pb} + \text{Hg})$  and  $^{207}\text{Pb}$ , which were measured for 40 ms) and a settling time of 1 ms for each isotope. Mass  $^{202}\text{Hg}$  was measured to monitor the  $^{204}\text{Hg}$  interference on  $^{204}\text{Pb}$  (using a  $^{202}\text{Hg}/^{204}\text{Hg}$ -ratio of 4.36). For net intensities for mass  $^{204}\text{Pb}$ , corrected for  $^{204}\text{Hg}$ , above the limit of detection these analyses were discarded in favour of performing a common Pb-correction. The laser induced elemental fractionation and the instrumental mass bias on measured isotopic ratios were corrected by matrix-matched external standardisation using the GJ-1 zircon standard (Jackson et al. 2004). Samples were analysed in sequences where six standards are analysed initially, followed by ten samples, followed by three standards, and then repeating ten unknowns followed by three standards.

The raw data were exported in ASCII format and processed using Excel-based in-house age data reduction spreadsheets. Age calculations for populations were carried out using the IsoPlot/Ex 3.0 excel add in (Ludwig 2003).

## Results

In the following LA-SF-ICPMS U-Pb zircon dating results are given for each sample analysed.  $^{207}\text{Pb}/^{206}\text{Pb}$  weighted mean ages were calculated using the Excel add-in IsoPlot/Ex version 3.0 (Ludwig 2003). All ages in the text are quoted with two sigma uncertainties. All tabulated age data are presented in Appendix 1. All data that are < 10% discordant are presented on  $^{206}\text{Pb}/^{238}\text{U}$ - $^{207}\text{Pb}/^{235}\text{U}$  Wetherill concordia diagrams. Error ellipses on diagrams are shown with one sigma uncertainties and where relevant  $^{207}\text{Pb}/^{206}\text{Pb}$  ages are shown on weighted mean age plots with two sigma uncertainty. The mean squared weighted deviates (MSWD) is used as a convenient measure of scatter in the data. An MSWD = 1 indicates that the scatter in the data is equal to that predicted from the analytical error. MSWD > 1 indicates greater scatter than would be predicted from analytical errors alone, whereas MSWD < 1 indicates less scatter than would be predicted from analytical errors alone. Thus MSWD significantly greater than 1 indicates that there is a real difference in ages of the grains analysed.

### 496513

Collector: Dave Coller

Lithology: Felsic sheet cutting dominant felsic orthogneiss immediately underlying supracrustal belt on central Storø.

Location: central east Storø

Locality: dcl2005-152, 64°27.812'N, -50°55.612'W

Aim: minimum age of gneissic banding in dominant felsic orthogneiss structurally underlying the supracrustal belt on Storø.

Age of emplacement: c. 2715 Ma? or 2981 Ma?

The zircons are typically 150–300 µm in length with aspect ratios 1:2 to 1:3, typically prismatic. Around half have CL-bright homogeneous or oscillatory-zoned cores, the remainder are CL-dull and fairly homogeneous. Those with CL-bright cores often have CL-dark homogeneous rims up to 60 µm wide.

Twenty-three spots in 23 grains were analysed. Seven analyses with high common Pb were discarded. The zircons have 42–910 ppm U and Th/U typically 0.22 to 1.25. The younger grains tend toward higher U contents. Sixteen concordant analyses give an age range of  $3136 \pm 27$  to  $2548 \pm 16$  Ma with no distinct age populations present. A cluster of four ages at c. 2981 Ma and also at 2715 Ma may represent the emplacement age, though this is unclear as neither can be linked to distinct zircon morphologies, and this supposition is based only on the relatively high proportions of grains of these ages represented.

This felsic sheet cuts the gneissic fabric in the dominant felsic orthogneiss on central north Storø. It may have been emplaced at either c. 2981 or 2715 Ma, though neither age is well-defined.

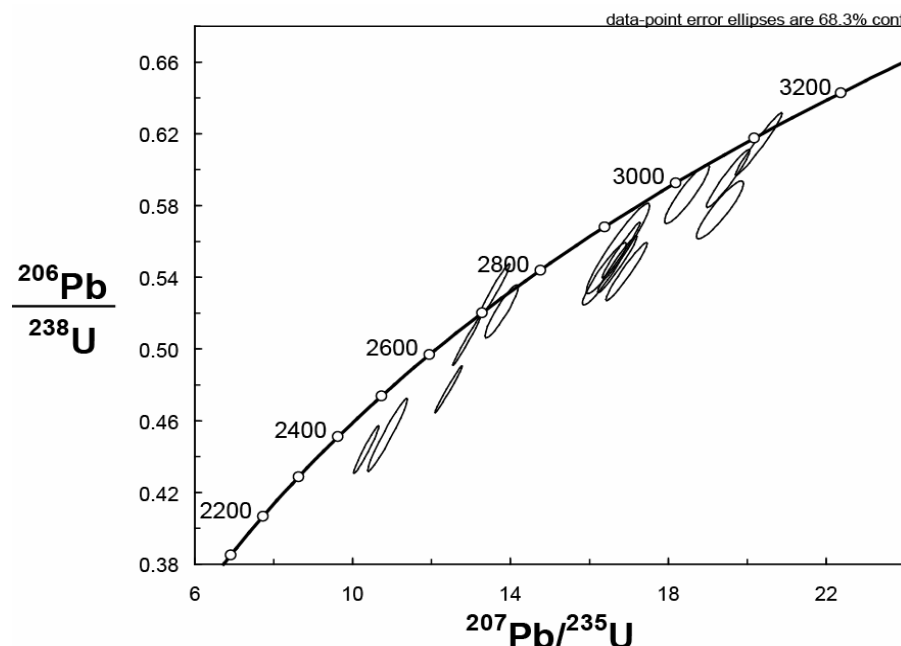


Figure 8. 496513  $^{206}\text{Pb}/^{238}\text{U}$ - $^{207}\text{Pb}/^{235}\text{U}$  concordia diagram.

**496516**

Collector: Dave Coller

Lithology: Felsic orthogneiss immediately north of the anorthosite on central Storø.

Location: central east Storø

Locality: dcl2005-186, 64°27.397'N, -50°58.346'W

Aim: emplacement age of dominant orthogneiss structurally underlying the supracrustal belt on central Storø

Age of emplacement:  $3045 \pm 13$  Ma (upper-intercept age, MSWD, 3.1, n = 16 of 25)

The zircons are typically 100–300  $\mu\text{m}$  in length with aspect ratios of 1:1 to 1:2 and commonly prismatic. Most show well-defined closely-spaced oscillatory zonation. A minority show sector zonation. Many grains have thin (up to 30  $\mu\text{m}$ ) CL-dull rims.

Twenty-five spots in 21 grains were analysed. Ages range from  $3060 \pm 13$  to  $2637 \pm 12$  Ma. Oscillatory-zoned cores have 16–100 ppm U and Th/U of 0.45–0.86. There is a trend toward lower Th/U for cores younger than c. 3020 Ma, and also for rim analyses, which reach a minimum of 0.05 for the youngest rim age. Sixteen oscillatory-zoned cores and one sector zoned core, all with relatively high Th/U, give a poorly defined age of  $3045 \pm 13$  Ma (upper-intercept age, MSWD, 3.1, n = 16 of 25). This age also agrees well with the most concordant (and therefore probably the most reliable) oscillatory zoned core analysis, which is  $3050 \pm 11$  Ma (0.4% discordant).

This sample was collected as representative of the dominant felsic orthogneiss structurally underlying the supracrustal belt on central east Storø. The data show it is a Mesoarchaean rock emplaced at c. 3050 Ma, based on analyses of oscillatory-zoned cores that appear to have undergone some degree of recrystallisation based on a trend toward lower Th/U with decreasing age.

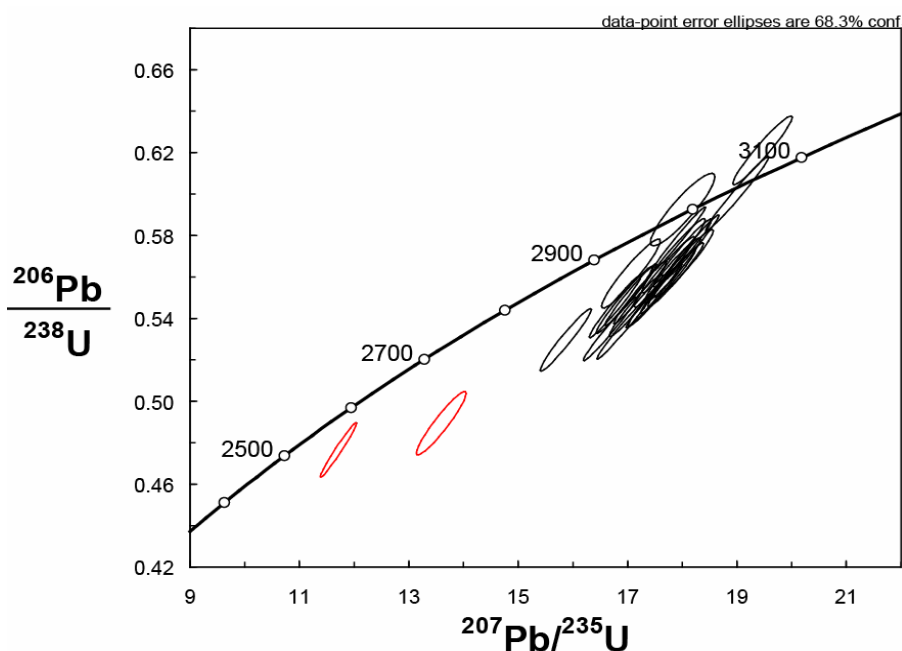


**Figure 9.** 496516  $^{206}\text{Pb}/^{238}\text{U}$ - $^{207}\text{Pb}/^{235}\text{U}$  concordia diagram.

## 496519

Collector: Dave Coller

Lithology: highly-deformed aplitic sheet within cataclastic rock, post-dating the onset of cataclastic deformation, within a broad zone of deformation on Sermitsiaq.

Location: Sermitsiaq

Locality: dcl2005-284, 64 18.289°N, -51 20.243°W

Aim: minimum age constraint on the onset of cataclastic deformation within the shear zone on Sermitsiaq.

Age of emplacement: ?  $\leq$  c. 2850 Ma (n = 5 of 8)

Age of metamorphism: c. 2670 Ma (n = 1 of 8)

This sample is dominated by completely metamict grains, on which LA-SF-ICPMS analysis was not attempted. The remaining few grains are typically 100–200  $\mu\text{m}$  in length with aspect ratios 1:1 to 1:3, commonly prismatic. They have weakly- to well-defined oscillatory zonation and a few have thin CL-dark rims.

Twelve spots in 9 grains were analysed. Four analyses with high common Pb were strongly discordant and were discarded. The zircons have 6–1307 ppm U, with a correlation between increasing U content with decreasing age. Ages range from  $3662 \pm 1968$  Ma (very low-U and Pb) to  $2670 \pm 25$  Ma (very high-U and Pb). The data fall into two main groups that are not strongly linked to distinct zircon morphologies. A single old grain produced the only two Eo- to Palaeoarchaean ages of  $3662 \pm 1968$  Ma and  $3551 \pm 26$  Ma. Five grains form a rough population at  $2853 \pm 36$  Ma (upper-intercept age, MSWD 3.8, n = 5 of 8). A single homogeneous grain has a much younger age of  $2670 \pm 25$  Ma and very high U (1307 ppm) and low Th/U of 0.09.

This highly-deformed aplitic sheet was collected from within a zone of cataclastic deformation within the shear zone on Sermitsiaq. The timing of emplacement of the dyke post-dates the onset of cataclasis as the dyke cross-cuts but is deformed by the cataclastic deformation. The timing of emplacement is not at all clear from the age data. The c. 2850 Ma age of the majority of the grains analysed (five grains) is not well-defined and these may also be inherited from metasedimentary rocks on Sermitsiaq known to carry detrital zircons of this age (see Hollis 2005). The single c. 3600 Ma grain is interpreted as inherited from rocks of the Itsaq gneiss complex, also present locally. The single 2670 Ma grain may represent the timing of emplacement as it has very high U (and low Th/U), typical of late-stage melts. It is possible that the dominant metamict grains (not analysed) – which are by inference high-U – are also this age. This age corresponds with the timing of known regional amphibolite facies metamorphism and partial melting (eg. Nutman et al. 1989, Friend et al. 1996, Hollis 2005).

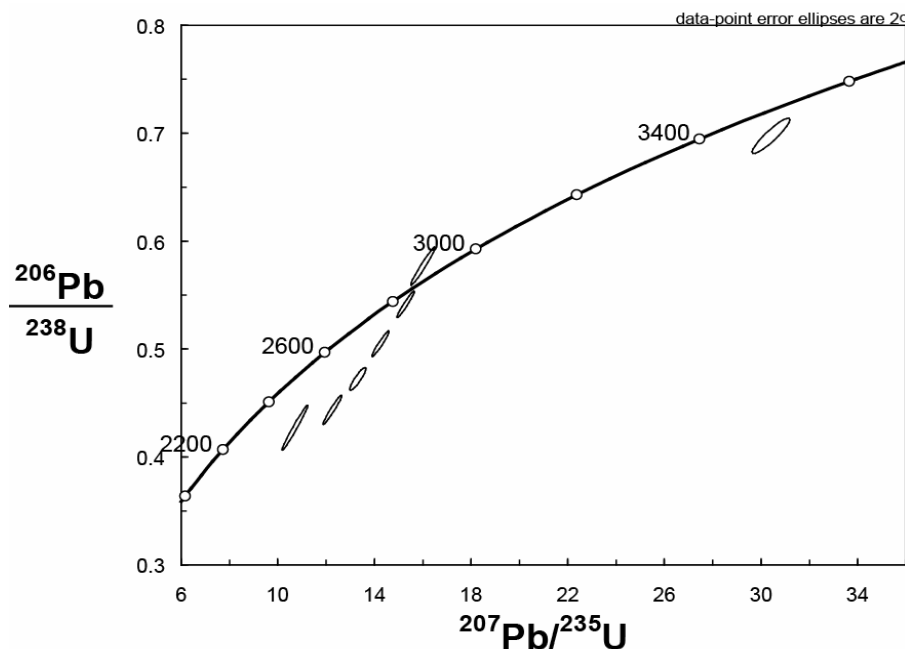


**Figure 10.** 496519  $^{206}\text{Pb}/^{238}\text{U}$ - $^{207}\text{Pb}/^{235}\text{U}$  concordia diagram.

#### 498420

Collector: Jeroen van Gool

Lithology: weakly-foliated biotite-bearing granodioritic to tonalitic gneiss

Location: Ujarassuit area 9

Locality: jvg2005-088, 64 53.202°N, -50 14.203°W

Aim: age of youngest phase of orthogneisses and maximum constraint on formation of regional F3 folds

Age of emplacement:  $\leq$  c. 2870 Ma

The zircons are 50–150  $\mu\text{m}$  with aspect ratios typically 1:2 to 1:3. All grains are homogeneous or show patchy zonation with indications of recrystallisation.

Twenty-one spots in 20 grains were analysed. Eight analyses with high common Pb were strongly discordant and were discarded. The zircons have 6–1307 ppm U with Th/U of 0.27–2.71. The data show a spread in ages from c. 2867 to 2764 Ma. The spread in ages do not show any correlation with chemistry or morphology.

The sample is representative of the youngest phase of felsic orthogneiss present in the Ujarassuit Nunaat – east region. This lithology holds a gneissic fabric, but post-dates the main phase of fabric formation in the regional felsic orthogneisses. Given the spread in age data it is possible that Pb-loss may have affected this sample after emplacement and that the oldest grain –  $2867 \pm 27$  Ma (< 2% discordant) – falls close to the emplacement age. Alternatively the oldest 3 grains, which fall away from the main age group, may be inherited and the cluster at c. 2780 Ma may reflect the timing of emplacement. Therefore the regional

gneissic fabric is constrained to being older than c. 2780 Ma, and the kilometre-scale F3 folding must be younger than at least c. 2870 Ma.

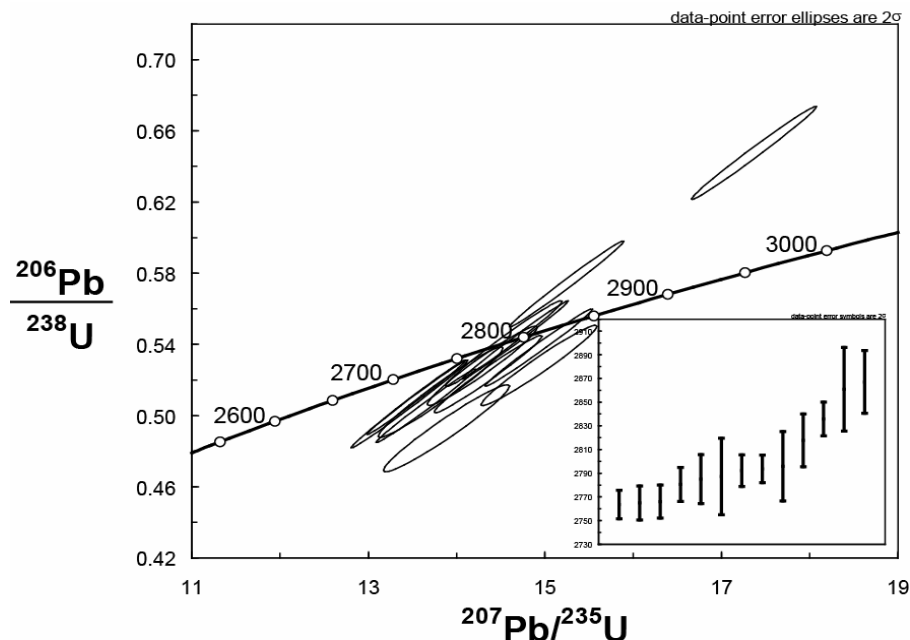


**Figure 11.** 498420  $^{206}\text{Pb}/^{238}\text{U}$ - $^{207}\text{Pb}/^{235}\text{U}$  concordia diagram and inset  $^{207}\text{Pb}/^{206}\text{Pb}$  age plot.

#### 498422

Collector: Jeroen van Gool

Lithology: homogeneous medium-grained hornblende gneiss, possibly originally a gabbro, which forms a part of the mafic amphibolite sequence, or is possibly a later intrusion

Location: Ujarassuit area 9

Locality: jvg2005-083, 64 53.353°N, -50 13.699°W

Aim: depositional or minimum age of the supracrustal sequence in Ujarassuit area 9

Age of metamorphism:  $2598 \pm 10$  Ma (MSWD 1.3, n = 5)

Only a few small zircons were obtained from this sample. They are 100–150  $\mu\text{m}$  in length with aspect ratios typically 1:1 to 1:2. All grains are homogeneous.

Six spots in 6 grains were analysed. None contained significant common Pb. Concordant ages (< 3% discordant, n = 5) range from  $2607 \pm 14$  to  $2566 \pm 9$  Ma with U contents of 260–749 ppm and Th/U of 0.02–0.11. Four of five analyses define a population with some significant spread in ages at  $2598 \pm 10$  Ma (weighted average, MSWD 1.3, n = 5).

The sample was collected from a homogeneous hornblende gneiss, possibly originally a gabbro, within the mafic amphibolite sequence in the Ujarassuit Nunaat–east area. The low Th/U and homogeneous morphologies are consistent with a  $2598 \pm 10$  Ma metamorphic age for this sample and therefore for the supracrustal belt as a whole.

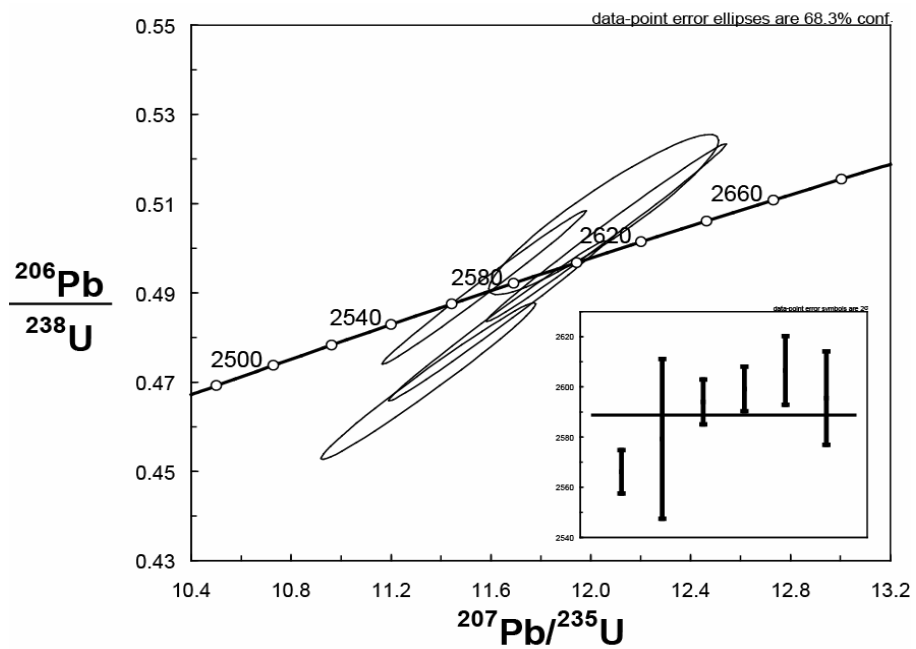


**Figure 12.** 498422  $^{206}\text{Pb}/^{238}\text{U}$ - $^{207}\text{Pb}/^{235}\text{U}$  concordia diagram and inset  $^{207}\text{Pb}/^{206}\text{Pb}$  age plot.

#### 498447

Collector: Jeroen van Gool

Lithology: Homogeneous hornblende-bearing quartz-dioritic gneiss that forms an integral part of the supracrustal unit (does not post-date the supracrustal rocks).

Location: Ujarassuit area 8

Locality: jvg2005-187, 64 57.044°N, -50 17.446°W

Aim: age of formation of (at least part) of the Ujarassuit Nunaat area 8 supracrustal belt

Age of metamorphism:  $2617 \pm 6$  Ma (upper-intercept age, MSWD 0.35, n = 12 of 17)

The zircons are 50–150 µm with aspect ratios typically 1:1 to 1:2.5. Approximately half of the grains have oscillatory-zoned cores with homogeneous rims (up to 30 µm wide). The remainder are completely homogeneous and commonly equant, consistent with growth during metamorphism.

Thirty spots in 30 grains were analysed. Eight analyses with high common Pb were discarded. Four oscillatory-zoned cores yielded ages between  $2936 \pm 34$  Ma and  $2707 \pm 14$  Ma with U contents of 99–237 ppm and Th/U of 0.25–0.98. The remaining 17 analyses – 16 homogeneous cores and one homogeneous rim – yielded ages from  $2671 \pm 18$  Ma to  $2581 \pm 11$  Ma with U contents of 79–265 ppm and Th/U of 0.06–0.18. These relatively low Th/U ratios, coupled with the distinct homogeneous morphologies, are consistent with zircon growth and/or recrystallisation during metamorphism. Thirteen of the 17 of these relatively young grains yield a population at  $2617 \pm 6$  Ma (upper-intercept age, MSWD 0.35, n = 12 of 17, 3 oldest and one youngest grain excluded), interpreted as the age of metamorphism.

The age of emplacement of this rock is not clear from the data available as the 4 cores yielded ages spanning the range  $2936 \pm 34$  Ma and  $2707 \pm 14$  Ma. It is possible that the youngest of these ages represents a mixed core-rim age and may therefore be geologically meaningless. The age of metamorphism of this rock is quite well-constrained to  $2617 \pm 6$  Ma, and correlates with amphibolite-facies metamorphism around this time known from the central Godthåbsfjord area and therefore influencing a wide region (eg. Hollis 2005). This is also consistent with the metamorphic age derived from sample 498422 (see above and Figs 1 and 2, area 9).

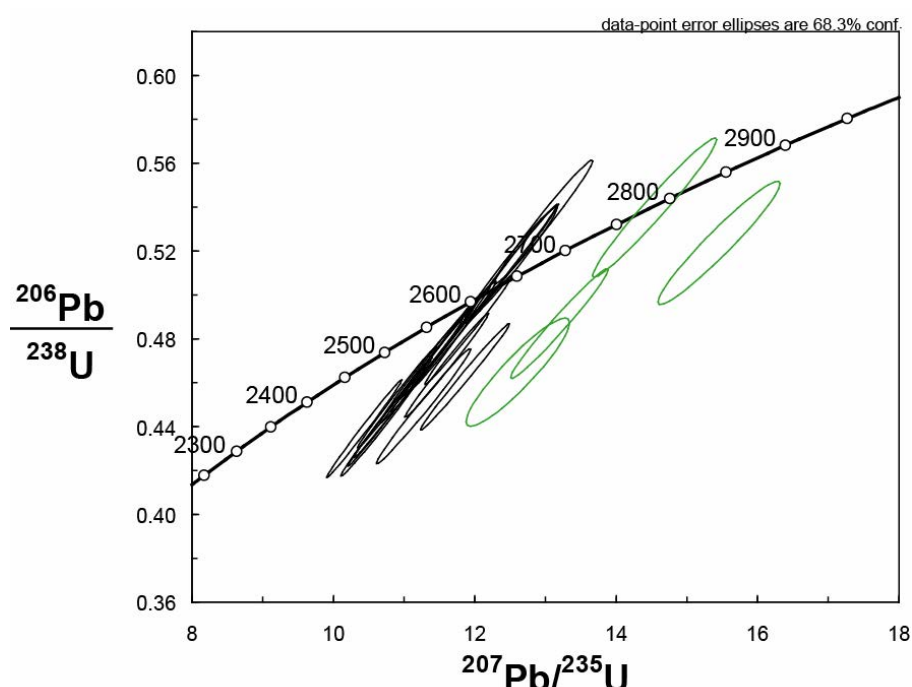


**Figure 13.** 498447  $^{206}\text{Pb}/^{238}\text{U}$ - $^{207}\text{Pb}/^{235}\text{U}$  concordia diagram and inset  $^{207}\text{Pb}/^{206}\text{Pb}$  age plot.

#### 498452

Collector: Jeroen van Gool

Lithology: Medium- to coarse-grained leucogranite intruded into amphibolitic supracrustal rocks in Ujarassuit area 8.

Location: Ujarassuit area 8

Locality: jvg2005-189, 64 57.082°N, -50 17.616°W

Aim: minimum age of formation of the supracrustal belt in Ujarassuit area 8 and minimum age of gneissic fabric preserved in the supracrustal rocks.

Age of emplacement:> c. 3010 Ma

The zircons are typically 50–100 µm with aspect ratios typically 1:2 to 1:3. Most grains have oscillatory-zoned cores, some with CL-dark homogeneous rims up to 60 µm wide.

Thirty-one spots in 27 grains were analysed. Nine analyses with high common Pb were discarded. The remaining 22 grains yield ages between  $3338 \pm 45$  Ma and  $2787 \pm 26$  Ma with U contents of 67–369 ppm and Th/U of 0.32 to 1.20. There is no significant correlation between zircon ages, chemistry, and morphology. Seven analyses of six oscillatory-zoned cores and one oscillatory-zoned rim form a cluster of ages at c. 3010 and another 7 ages for oscillatory-zoned and homogeneous cores range from 3026–3077 Ma with significant spread in the data. Two older core analyses of  $3338 \pm 45$  Ma and  $3141 \pm 57$  Ma may be inherited grains. A single analysed homogeneous rim gives an age of  $2787 \pm 26$  Ma.

This is a sample of a leucogranite intrusive into amphibolitic supracrustal rocks (of possibly volcanic origin) within Ujarassuit area 8. The age population at c. 3010 Ma defined by 7 analyses may represent a real geological event, or may alternatively represent Pb-loss from older grains, given the significant spread in ages for another 7 grains from 3026–3077 Ma. We therefore interpret the c. 3010 Ma age as a minimum age of emplacement. The data provide a minimum constraint on the age of deposition of the supracrustal belt of  $\geq$  c. 3010 Ma.

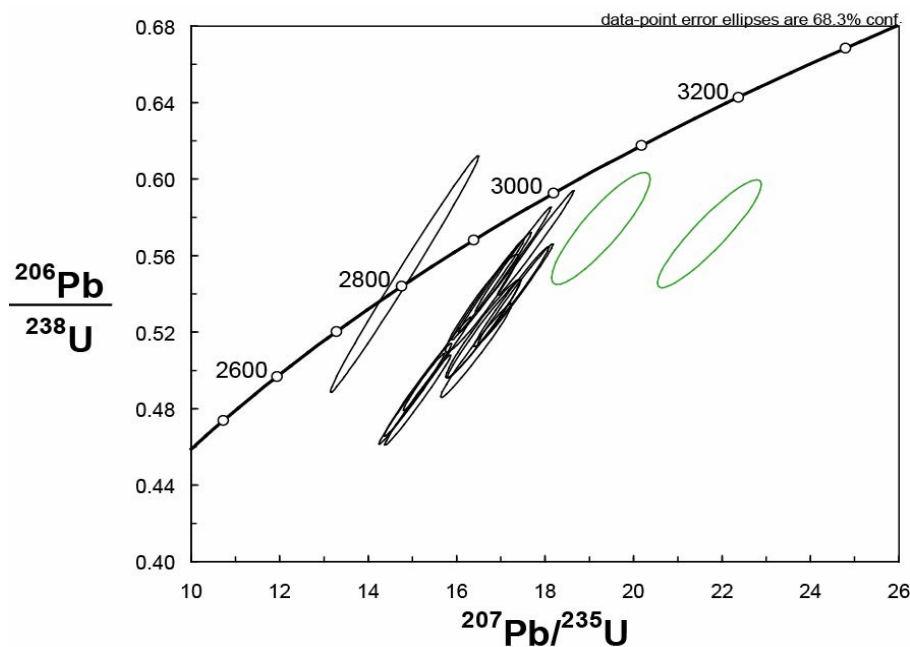


**Figure 14.** 498452  $^{206}\text{Pb} / ^{238}\text{U}$ - $^{207}\text{Pb} / ^{235}\text{U}$  concordia diagram.

#### 498481

Collector: Jeroen van Gool

Lithology: late aplitic dyke within Tasersuaq pluton representing the last intrusive phase

Location: Ujarassuit area 6, Tasersuaq pluton

Locality: jvg2005-287, 64 58.741°N, -50 25.764°W

Aim: minimum age of deformation of the Tasersuaq pluton

Age of emplacement: ?  $2936 \pm 13$  Ma (MSWD 3.5, n = 5 of 6)

This sample yielded very few zircons, all of which are  $\leq 100 \mu\text{m}$  in length, with aspect ratios of typically 1:2 and prismatic. All are oscillatory-zoned and four of the five grains give a quite dark CL response, while the last has a bright CL response.

Six spots in 7 grains were analysed. One analysis with high common Pb was discarded. The four CL-dark grains give a rough age population of  $2936 \pm 13 \text{ Ma}$  (MSWD 3.5,  $n = 5$  of 6) with U contents of 265–469 ppm and Th/U of 0.48–1.68. The one CL-bright grain is  $2808 \pm 14 \text{ Ma}$  with relatively low U content (65 ppm) and Th/U (0.39).

The sample was collected from a late aplitic dyke that post-dates all deformation in the Tasersuaq pluton and thus provides a minimum age constraint on deformation. There are too few zircon grains from this sample to place much emphasis on the inferred age constraints, and also some ambiguity in the age data itself. It is probable that the four  $2936 \pm 13 \text{ Ma}$  grains represent the timing of emplacement of the dyke, though the age is poorly constrained. If so, this would indicate that no further deformation events affected the Tasersuaq pluton after c. 2936 Ma, consistent with the findings of Garde et al. (2000).

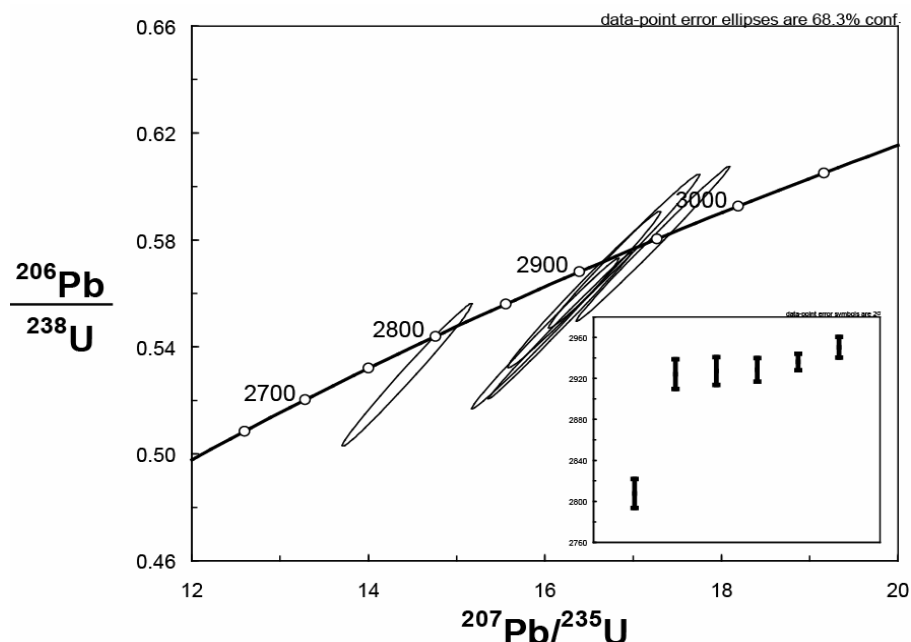


**Figure 15.** 498481  $^{206}\text{Pb}/^{238}\text{U}$ - $^{207}\text{Pb}/^{235}\text{U}$  concordia diagram and inset  $^{207}\text{Pb}/^{206}\text{Pb}$  age plot.

**498496**

Collector: Jeroen van Gool

Lithology: Strongly deformed homogeneous light grey tonalitic biotite orthogneiss, which is discordant to an older gneissic fabric

Location: Ujarassuit area 6

Locality: jvg2005-316, 64 58.193°N, -50 23.122°W

Aim: Timing of relatively young phase of tonalitic magmatism

Age of emplacement:  $\geq 2750$  Ma

The zircons are 100–200  $\mu\text{m}$  in length with aspect ratios typically 1:3 to 1:4, and prismatic. A few have metamict cores and all are CL-dark. BSE imaging shows that most have oscillatory zonation or relict oscillatory zonation. Many have concentric and radial fracturing around high-U cores. Some of these fractures show partial recrystallisation features. The majority are homogeneous, a few with some poorly-defined oscillatory zonation and a few with wide BSE bright rims around darker cores.

Thirty spots in 28 grains were analysed. Nineteen with high common Pb were discarded. The high proportion of analyses showing high common Pb is attributed to the high degree of metamictisation (high-U). Of the remaining 11 analyses ages range from  $2969 \pm 16$  to  $2691 \pm 58$  Ma, with U contents of 65–1183 ppm and Th/U of 0.12–0.91. The three oldest grains are  $2969 \pm 16$ ,  $2963 \pm 95$ , and  $2878 \pm 55$  Ma. Eight younger grains form a cluster of ages with significant spread at c. 2750 Ma. The youngest grain, at  $2691 \pm 58$  Ma, is by far the most U-rich.

The sample is representative of the youngest phase of magmatism recognised in the Ujarassuit region. This lithology post-dates formation of the main gneissic fabric in the dominant regional felsic gneisses and is deformed by the kilometre-scale F3 folds. It is possible that the poorly defined c. 2750 Ma age represents the timing of emplacement, though this is far from clear from the data. It does, however, give a minimum age constraint on the timing of emplacement age and on the development of the regional gneissic fabric, and a maximum constraint on the timing of regional F3 folding.

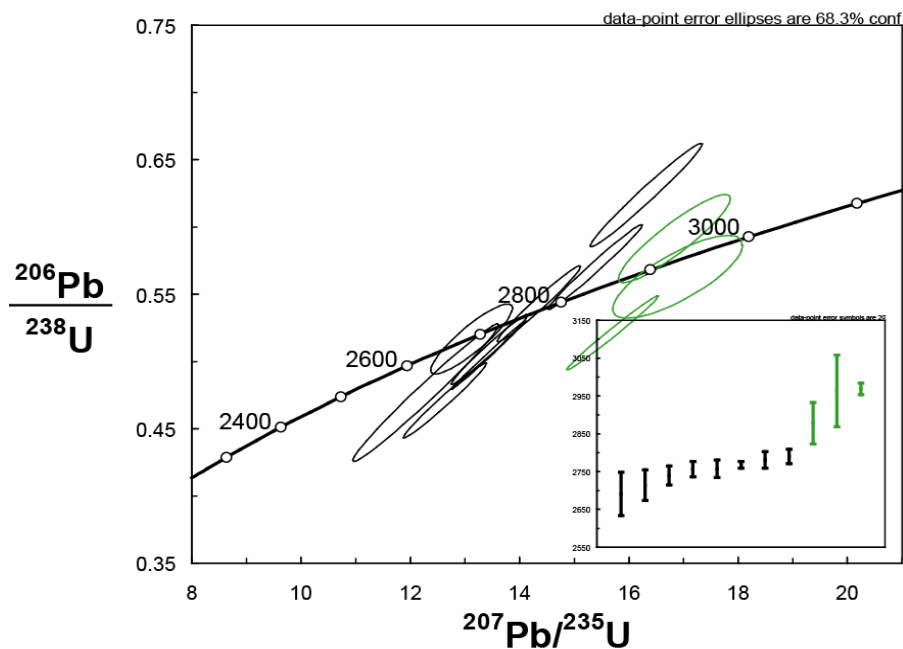


**Figure 16.** 498496  $^{206}\text{Pb}/^{238}\text{U}$ - $^{207}\text{Pb}/^{235}\text{U}$  concordia diagram and inset  $^{207}\text{Pb}/^{206}\text{Pb}$  age plot.

#### 498497

Collector: Jeroen van Gool

Lithology: foliated pegmatite that postdates the main gneissic fabric in the regionally-dominant orthogneiss and which is deformed by a subsequent shear-fabric.

Location: Ujarassuit area 6

Locality: jvg2005-317, 64 58.184°N, -50 23.765°W

Aim: minimum age constraint on formation of main regional gneissic fabric and maximum constraint on later phase/s of regional deformation

Age of emplacement:  $\geq$  c. 2645 Ma

The zircons are 80–150  $\mu\text{m}$  in length with aspect ratios typically 1:1 to 1:3, and commonly prismatic. Approximately one third are homogeneous, the remainder showing metamict and/or patchy heavily recrystallised cores.

Twenty spots in 20 homogeneous grains were analysed. Seven analyses with high common Pb were discarded. Ages range from  $2593 \pm 22$  to  $2765 \pm 23$  Ma with U contents of 221–1115 ppm and Th/U of 0.05–0.37. Six grains (not morphologically distinct) form a cluster of ages at c. 2645 Ma, however there is significant spread in the whole dataset.

The sample was collected from a pegmatite that post-dates the main gneissic fabric in the regionally dominant felsic gneisses, but which is also affected by later deformation. There is no significant relationship between zircon morphology and age data, nor with chemistry. As such the significant spread in age data is difficult to interpret. The youngest age group – c. 2645 Ma – can therefore be interpreted only as a minimum estimate of the age of em-

placement, which could have occurred significantly earlier. Therefore development of the main gneissic fabric is constrained to > c. 2645 Ma.

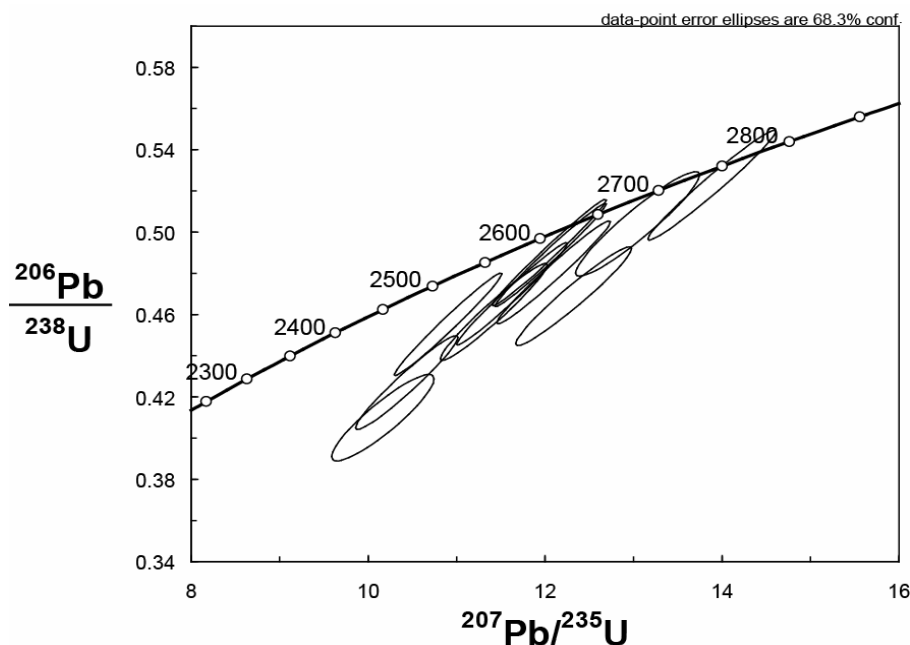


**Figure 17.** 498497  $^{206}\text{Pb}/^{238}\text{U}$ - $^{207}\text{Pb}/^{235}\text{U}$  concordia diagram and inset  $^{207}\text{Pb}/^{206}\text{Pb}$  age plot.

#### 498762

Collector: Jeroen van Gool

Lithology: Homogeneous tonalitic leucogneiss intrusive into supracrustal rocks, and representative of the dominant felsic orthogneisses in this area

Location: Ujarassuit area 6

Locality: jvg2005-294, 64 58.544°N, -50 24.344°W

Aim: emplacement age of dominant regional orthogneiss in area 6.

Minimum age of emplacement:  $\geq 3025$  Ma

The zircons are 50–200 µm with aspect ratios typically 1:1.5 to 1:3, and prismatic. They commonly show oscillatory zonation. A few have metamict zones, often showing concentric and radial zonation with varying degrees of recrystallisation of fractures. A few have thin (up to 30 µm) homogeneous rims.

Thirty spots in 29 grains were analysed. Five analyses with high common Pb were discarded. Ages range from  $3155 \pm 31$  Ma to  $2706 \pm 41$  Ma, with U contents of 9–501 ppm and Th/U of 0.04–0.45. There is slight tendency toward lower Th/U and higher U contents with decreasing age, possibly indicative of some metamorphic recrystallisation of older grains, which is supported by morphological indications of recrystallisation and partial metamictisation. Around half of the analyses form a cluster of ages at c. 3025 Ma, though these grains are not morphologically or chemically distinct from the remaining grains, and thus the significance of this group is difficult to assess.

This sample is representative of the dominant regional tonalitic leucogneiss, which in this location is intrusive into supracrustal rocks in Ujarassuit area 6. A cluster of ages at c. 3025 Ma may represent the emplacement age, with older grains reflecting inheritance, though this is not certain. Alternatively emplacement may have occurred earlier and some Pb-loss may have occurred, producing the younger population at c. 3025 Ma. This is therefore a minimum age of emplacement for the igneous precursor to this orthogneiss, with the possibility that slightly older ages ( $3155 \pm 31$  to  $3054 \pm 45$  Ma) may be closer to the original age of emplacement. The minimum age of emplacement is consistent with the supracrustal belt in Ujarassuit area 6 being of a similar age to the Ivisaartoq supracrustal belt (eg. Friend and Nutman 2005).

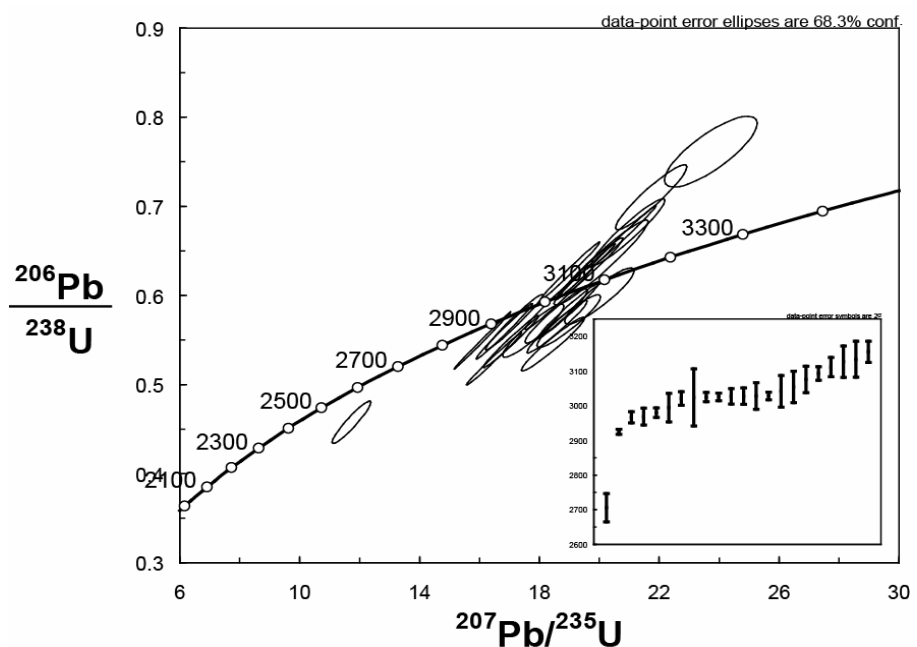


**Figure 18.** 498762  $^{206}\text{Pb}/^{238}\text{U}$ - $^{207}\text{Pb}/^{235}\text{U}$  concordia diagram and inset  $^{207}\text{Pb}/^{206}\text{Pb}$  age plot.

#### 498803

Collector: Nigel Kelly

Lithology: Migmatitic garnet-biotite schist with centimetre-scale interlayering of leucosome and leucocratic zones with more biotite-rich material. Of inferred sedimentary or volcanic origin

Location: Ujarassuit area 1

Locality: nmk2005-018, 64 50.622°N, -50 12.786°W

Aim: age of detrital or volcanic zircon and therefore age of deposition

Age of deposition: > 2609 Ma

Age of metamorphism/migmatisation:  $2609 \pm 14$  Ma (upper-intercept age, MSWD 2.3, n = 16)

The zircons are quite small, 80–120 µm in length with aspect ratios of typically 1:1 to 1:1.5. They are commonly rounded with slightly scalloped edges, suggestive of partial resorption. All are completely homogeneous.

Thirty spots in 30 grains were analysed. One analysis with high common Pb was discarded. Ages that are < 10% discordant ( $n = 16$ ) range from  $2625 \pm 11$  Ma to  $2553 \pm 15$  Ma with U contents of 669–1302 and Th/U of 0.44–1.41. There is significant spread in the age data with ages trending toward a plateau around 2575 Ma. All sixteen analyses yield a poorly-defined age of  $2609 \pm 14$  Ma (upper-intercept age, MSWD 2.3,  $n = 16$ ).

The sample was collected from a migmatitic garnet-biotite schist with interlayered leucosome and more biotite-rich material of inferred sedimentary or volcanic origin. Given the homogeneous rounded morphology of the grains, the  $2609 \pm 14$  Ma age is interpreted as a recrystallisation event, probably recording the timing of migmatitisation, rather than recording any origin detrital or volcanic age.

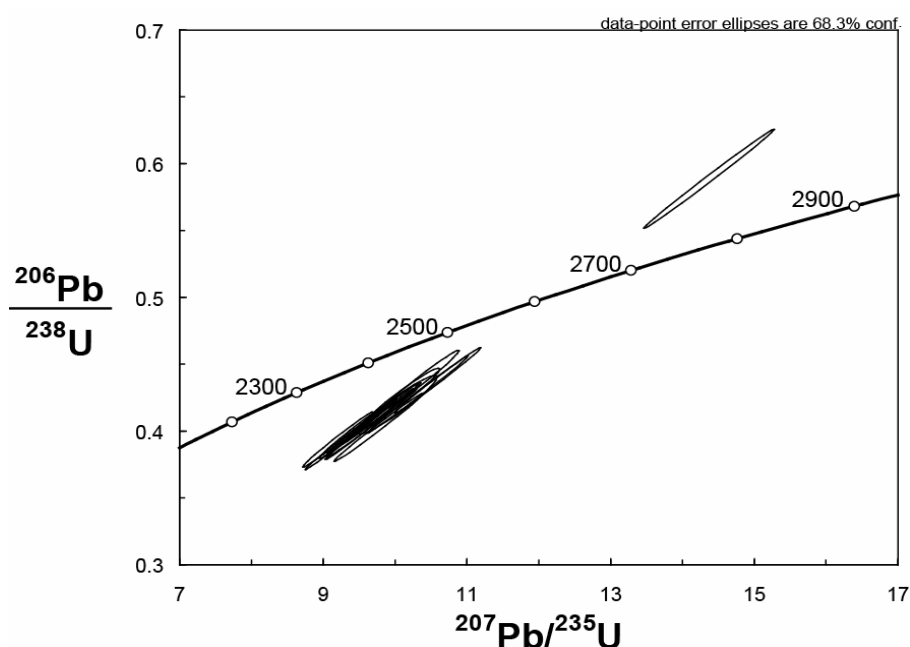


**Figure 19.** 498803  $^{206}\text{Pb}/^{238}\text{U}$ - $^{207}\text{Pb}/^{235}\text{U}$  concordia diagram and inset  $^{207}\text{Pb}/^{206}\text{Pb}$  age plot.

#### 498864

Collector: Nigel Kelly

Lithology: Heterogeneous migmatitic biotite-felsic orthogneiss. Granodioritic to dioritic layer, possibly pre-dating the tonalitic phase (cut by tonalite in some outcrops), with minor leucosome

Location: Ujarassuit area 4

Locality: nmk2005-195, 64 48.696°N, -50 24.414°W

Aim: age of earliest phase of magmatism within the regionally dominant felsic orthogneiss

Age of emplacement  $\geq 2974$  Ma

The zircons are 150–250  $\mu\text{m}$  in length with aspect ratios typically 1:2 to 1:3, and commonly prismatic. All have well-defined oscillatory zonation, a few with large homogeneous cores.

Thirty spots in 29 grains were analysed. No grains showed significant common Pb. Ages that are < 10% discordant ( $n = 26$ ) range from  $2974 \pm 13$  Ma to  $2699 \pm 14$  Ma with U contents of 19–448 and Th/U of 0.10–0.57. There is a slight trend toward lower Th/U with decreasing age. The age data show significant spread with no obvious plateau defining a distinct population.

The sample was collected from a granodioritic to dioritic layer within a heterogeneous migmatitic biotite-felsic orthogneiss, representative of the dominant regional orthogneiss in Ujarassuit area 4. This granodioritic to dioritic variety is commonly cut by the tonalitic phase of this gneiss and is interpreted as representative of the earliest phase of magmatism represented in this multi-component gneiss. The age data does not clearly define the age of emplacement. It is likely that some of the 6 ages represent partial Pb-loss from older grains, though there is no morphological or chemical evidence to support this. A cluster of ages at c. 2930–2870 Ma may encompass the timing of emplacement. A minimum constraint on the timing of emplacement is given by the oldest near-concordant grain –  $2974 \pm 13$  Ma (< 4% discordant).

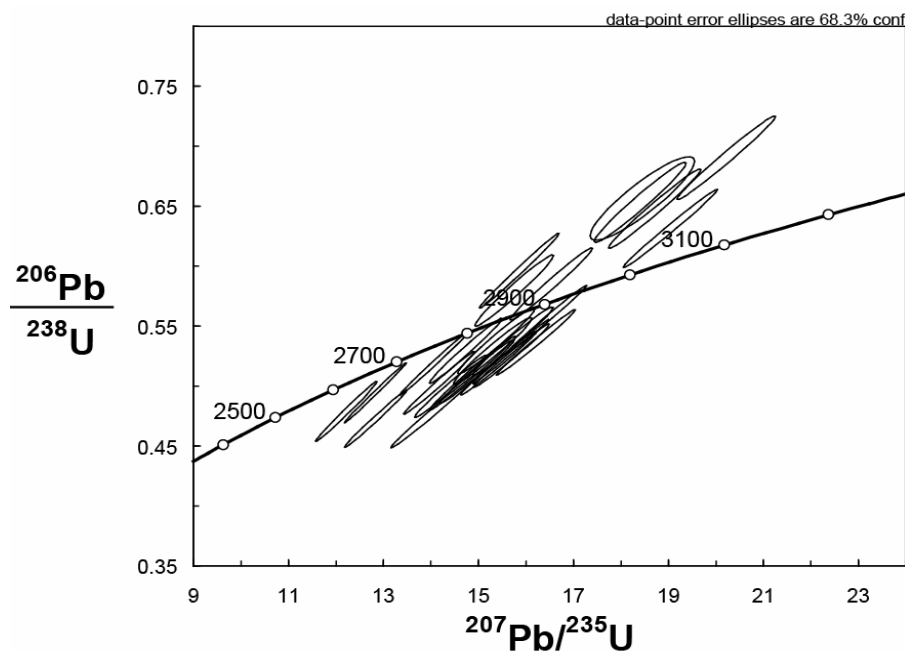


**Figure 20.** 498864  $^{206}\text{Pb}/^{238}\text{U}$ - $^{207}\text{Pb}/^{235}\text{U}$  concordia diagram.

**498877**

Collector: Nigel Kelly

Lithology: massive, weakly foliated felsic biotite orthogneiss with minor leucosome. Representative of the youngest phase of magmatism, post-dating the main gneissic fabric in the regionally dominant felsic orthogneisses

Location: Ujarassuit area 4

Locality: nmk2005-248, 64 49.638°N, -50 24.744°W

Aim: age of emplacement of youngest phase of magmatism in area 4

Age of emplacement:  $\geq$  c. 2825 Ma

The zircons are 50–150  $\mu\text{m}$  with aspect ratios typically 1:1 to 1:2.5, commonly prismatic. All have oscillatory zonation, a few with large sector-zoned cores.

Thirty spots in 29 grains were analysed. Two analyses with high common Pb were discarded. Ages that are  $< 10\%$  discordant ( $n = 26$ ) range from  $2845 \pm 31$  Ma to  $2672 \pm 14$  Ma with U contents of 28–1075 ppm and Th/U of 0.06–0.29. There is significant spread in the age data with no distinct plateau in ages.

The sample was collected from a massive, weakly foliated felsic biotite orthogneiss with minor leucosome. This is thought to be representative of the youngest phase of magmatism, post-dating the main gneissic fabric in the regionally dominant felsic orthogneisses. Unfortunately there is significant spread in the ages with no distinct correlation between ages, chemistry, and morphology. It is possible that ancient Pb-loss has affected grains of  $\geq 2780$  Ma. The two oldest grains are distinct high-U oscillatory-zoned cores that may be inherited. Ignoring these, the oldest near-concordant oscillatory-zoned core is  $2826 \pm 41$  Ma ( $< 0.9\%$  discordant), interpreted as the minimum timing of emplacement. This in turn gives a minimum constraint on the formation of the regional gneissic fabric.

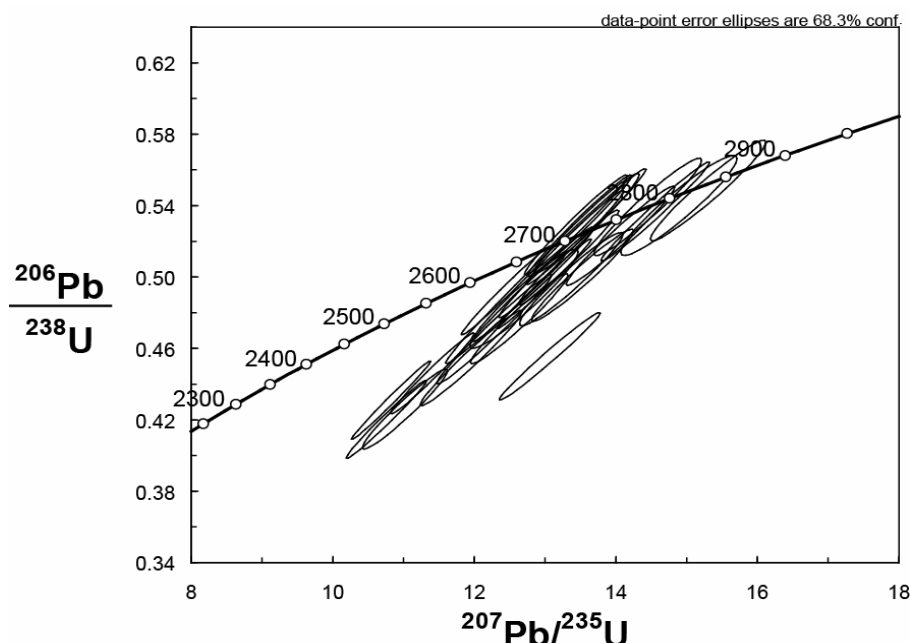


**Figure 21.** 498877  $^{206}\text{Pb}/^{238}\text{U}$ - $^{207}\text{Pb}/^{235}\text{U}$  concordia diagram.

**498892**

Collector: Nigel Kelly

Lithology: Coarse-grained, intermediate composition foliated amphibolite of inferred volcanic origin.

Location: Ujarassuit area 4

Locality: nmk2005-264, 64 48.396°N, -50 24.912°W

Aim: depositional age of volcanic supracrustal rocks

Age of deposition: ? c. 3400 Ma

The zircons are 50–150 microns long, with aspect ratios of 1:1 to 1:2 with stubby irregular shapes, consistent with a volcanic origin. Many have metamict cores, patchy zonation, and are heavily fractured. A few preserve relict oscillatory zonation.

Twenty-five spots in 25 grains were analysed. Two analyses with high common Pb were discarded. Ages range from c. 3440 Ma to 3029 Ma, though most are significantly discordant (> 5%). U contents range from 172–730 ppm and Th/U from 0.11–2.84. There is no significant correlation between age, chemistry, and morphology. The oldest 11 grains range from  $3440 \pm 8$  Ma to  $3228 \pm 16$  Ma, whereas the youngest three form a cluster at c. 3030 Ma, which may or may not reflect a real geological event.

The sample was collected from a coarse-grained, foliated amphibolite of intermediate composition and inferred to have a volcanic origin. The zircon morphologies (small, irregular grains) are consistent with a volcanic origin. The rock was evidently formed in the early part of the Mesoarchaean, though the exact depositional age is unclear. Given the spread in ages and cluster of ages at c. 3030 Ma, it seems likely that this sample has been affected by some Pb-loss. It is therefore difficult to assess the original depositional age, other than to say that this occurred prior to c. 3030 Ma. If the cluster of ages at c. 3400 Ma are close to the true depositional age, this would be an unusual result – supracrustal rocks of this age are otherwise unknown in the Nuuk region. However, we reiterate that the exact timing of deposition is not clear from the age data.

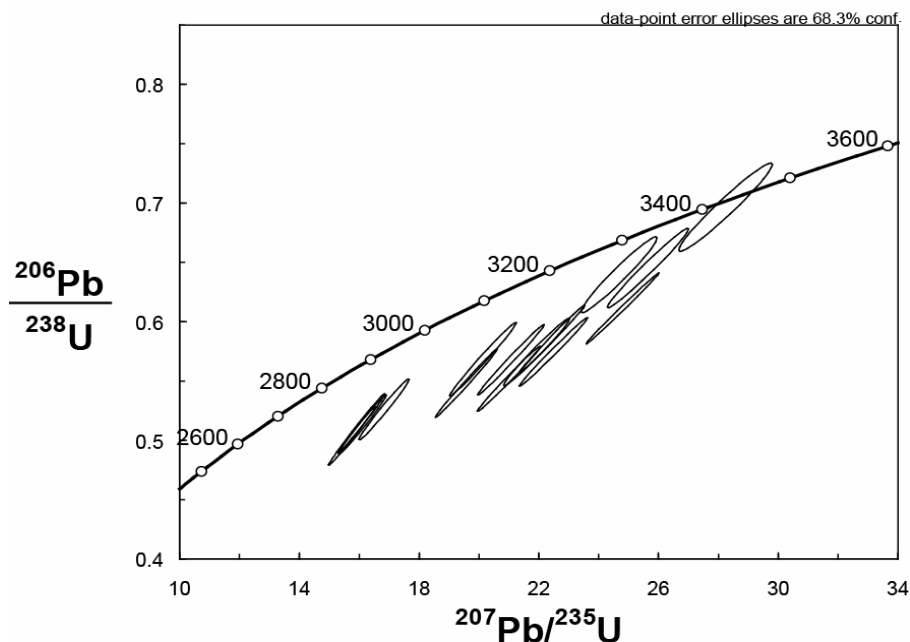


**Figure 22.** 498892  $^{206}\text{Pb}/^{238}\text{U}$ - $^{207}\text{Pb}/^{235}\text{U}$  concordia diagram and inset  $^{207}\text{Pb}/^{206}\text{Pb}$  age plot.

#### 498921

Collector: Nigel Kelly

Lithology: Felsic-intermediate biotite orthogneiss with minor leucosome

Locality: nmk2005-336, 64 45.918°N, -50 32.310°W

Location: Ujarassuit area 5

Aim: emplacement age of felsic orthogneiss dominant in Ujarassuit area 5

Age of emplacement:  $\geq$  c. 3373 Ma

The zircons are 100–200  $\mu\text{m}$  in length with aspect ratios typically 1:1 to 1:2.5, and commonly prismatic. The majority show oscillatory zonation, though some show patchy zonation and a few are homogeneous.

Thirty spots in 30 grains were analysed. No analyses had significant common Pb. Ages that are  $< 10\%$  discordant ( $n = 29$ ) range from c. 3373 to 3271 Ma with U contents of 42–620 ppm and Th/U of 0.02–1.21. There is no significant correlation between age, chemistry, and morphology. There is significant spread in the age data with no distinct plateau in ages.

The sample was collected from a felsic to intermediate biotite orthogneiss with minor leucosome, representative of the dominant orthogneiss in Ujarassuit area 5. The spread in ages from c. 3373 to 3271 Ma is probably the result of some ancient Pb-loss, though the timing of this event is not clear from the data. The oldest near-concordant grain –  $3373 \pm 16$  Ma ( $< 7.2\%$  discordant) – gives a minimum constraint on the timing of emplacement. This unit was previously mapped (Chadwick and Coe 1988) as Nûk gneiss, though it is clearly

significantly older. If c. 3370 Ma represents an emplacement age for this rock, this is unusual age for the Nuuk region. The only other thermal event recorded around this time is the emplacement of the Ameralik dyke swarms at c. 3510 to 3260 Ma (Nutman et al. 2004).

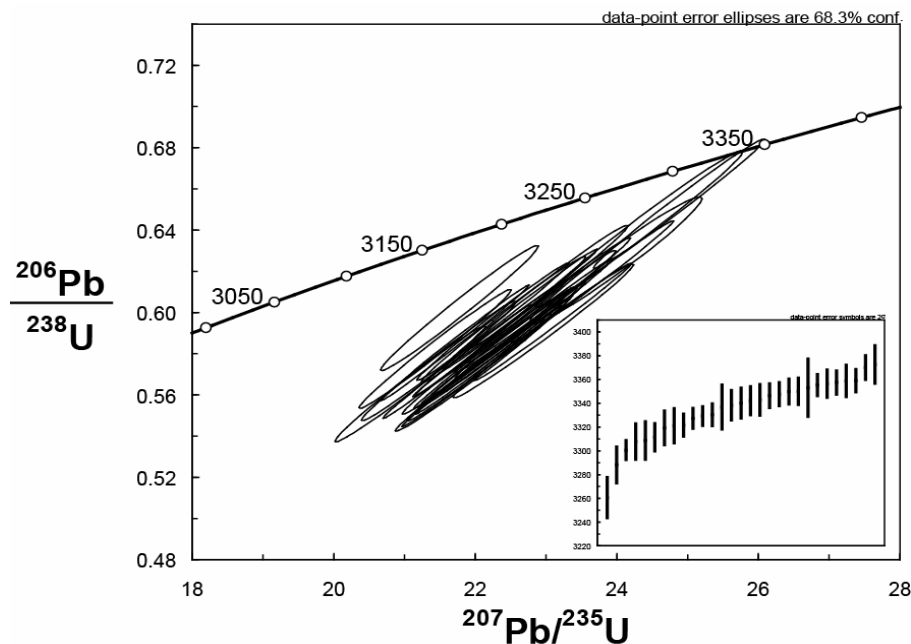


**Figure 23.** 498921  $^{206}\text{Pb}/^{238}\text{U}$ - $^{207}\text{Pb}/^{235}\text{U}$  concordia diagram and inset  $^{207}\text{Pb}/^{206}\text{Pb}$  age plot.

#### 498937

Collector: Nigel Kelly

Lithology: Felsic biotite orthogneiss with minor leucosome

Location: Ujarassuit area 5

Locality: nmk2005-351, 64 46.008°N, -50 29.664°W

Aim: age of emplacement of regionally dominant felsic orthogneiss in Ujarassuit area 5

Age of emplacement:  $3872 \pm 43$  Ma (upper-intercept age, MSWD 2.5, n = 12)

The zircons are 100–300 µm in length with aspect ratios typically 1:2 to 1:3, and commonly prismatic. Many of the grains show very distinct oscillatory zonation, some with broad homogeneous rims. A few grains show only relict oscillatory zonation and some are completely homogeneous.

Thirty spots in 27 grains were analysed. One analysis had significant common Pb and was discarded. Ages that are < 10% discordant (n = 23) range from c. 4000 to 3640 Ma with U contents of 36–387 ppm and Th/U of 0.15–0.97. There is no significant correlation between age, chemistry, and morphology. There is a cluster of ages at c. 3870 Ma (based on an upper-intercept of  $3872 \pm 43$  Ma (MSWD 2.5, n = 12) with a spread toward younger ages, the youngest being a homogeneous rim analysis. Five relatively older grains give an upper-intercept age of  $4009 \pm 18$  Ma (MSWD 1.4, n = 5).

The sample was collected from a felsic biotite orthogneiss with minor leucosome representative of the dominant felsic orthogneiss in Ujarassuit area 5. This was previously mapped as a part of the Eo- to Palaeoarchaean group of orthogneisses, which is also evident from the age data presented here. The precursor to this orthogneiss was likely emplaced at c. 3870 Ma with zircon grains partially affected by Pb-loss. A single homogeneous rim analysis giving an age of c. 3644 Ma may reflect a known regional metamorphic/migmatitic event at this time: granulite facies metamorphism of Eoarchaean gneisses is known to have occurred at c. 3650 Ma regionally (Nutman et al. 1996). Interestingly there are five very old grains in this sample, giving a reasonable upper-intercept age of  $4009 \pm 18$  Ma. Zircon older than 3900 Ma are very rare in the Nuuk region.

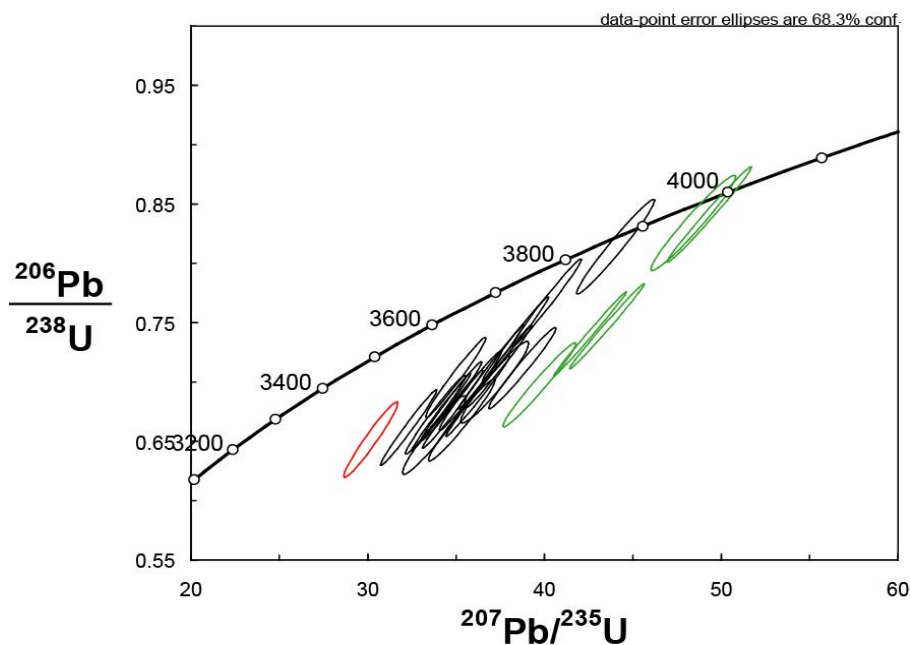


**Figure 24.** 498937  $^{206}\text{Pb}/^{238}\text{U}$ - $^{207}\text{Pb}/^{235}\text{U}$  concordia diagram and inset  $^{207}\text{Pb}/^{206}\text{Pb}$  age plot.

#### 498945

Collector: Nigel Kelly

Lithology: Medium to coarse-grained garnet-bearing amphibolite of inferred volcanic origin

Location: Ujarassuit area 5

Locality: nmk2005-369, 64 46.662°N, -50 30.720°W

Aim: age of deposition of volcanic supracrustal rock

Age of volcanic deposition: c. 3400 Ma

Age of metamorphism:  $3056 \pm 5$  Ma (MSWD 1.18, n = 5 of 39)

The zircons are 80–150 µm in length with aspect ratios of 1:1 to 1:2, commonly irregular to prismatic. All have the same distinct morphology. They have CL-bright homogeneous cores and CL-dark thin rims (up to 30 µm wide). The unusual contrast in CL and the consistency in morphology of all grains suggests a common origin for these grains (eg. formed in the same volcanic episode).

Forty-eight spots in 44 grains were analysed. Five analyses had significant common Pb and were discarded. Concordant ages ( $n = 39$ ) range from  $3472 \pm 26$  Ma to  $3050 \pm 13$  Ma with U contents of 18–118 ppm and Th/U of 0.01–2.37. There is a strong correlation between decreasing Th/U with decreasing age. Five analysis of rims give a fairly well-defined age of  $3056 \pm 5$  Ma (upper-intercept age anchored at the origin, MSWD 1.18,  $n = 5$ ). All have relatively high-U (88–132 ppm) and low Th/U (0.01–0.04), consistent with a metamorphic origin. The remaining analyses of homogeneous, oscillatory-zoned, and patchily-zoned cores form no distinct plateau in ages, but rather a range from c. 3472 to 3094 Ma.

The sample was collected from a garnet-bearing amphibolite of inferred volcanic origin in the Ujarassuit area 5. The range in ages, despite the similarity in morphology of all grains, and the strong correlation between Th/U and age are consistent with Pb-loss of the original zircon population during a later thermal event. The most concordant old grain is  $3417 \pm 16$  Ma (< 4.6% discordant), which is probably close to the original depositional age of at least part of the supracrustal belt in Ujarassuit area 5 (see Figs 1 and 4). The trend in younger ages toward c. 3050 Ma, corresponding decrease in Th/U, and the high-U, low Th/U population of rim analyses at  $3056 \pm 5$  Ma suggest that a thermal event at this time may have been responsible partial Pb-loss from the original volcanic population. This may be related to emplacement of regional felsic orthogneisses of this age (eg. Nûk gneisses, c. 3010–3070 Ma).

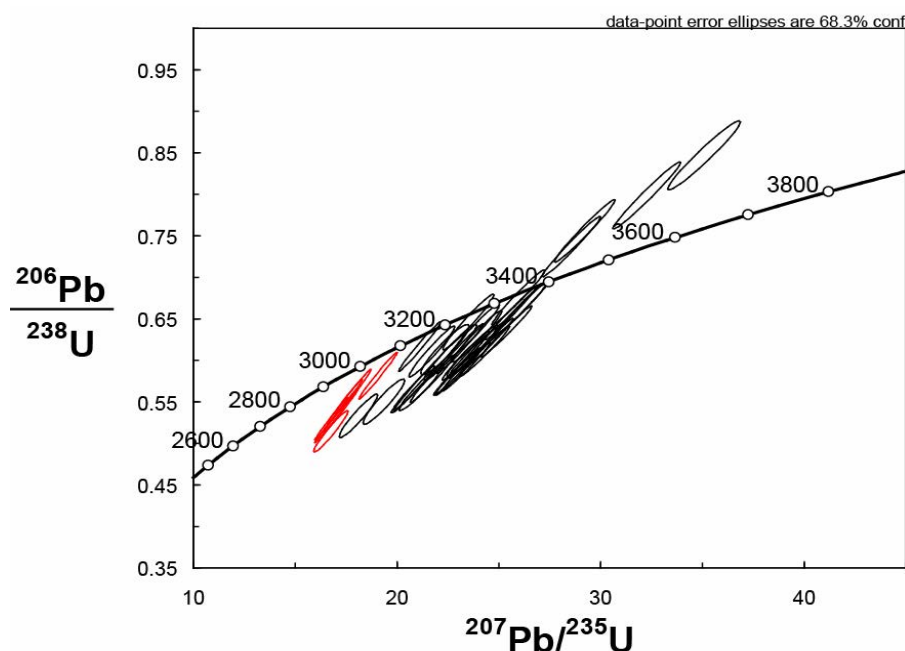


**Figure 25.** 498945  $^{206}\text{Pb}/^{238}\text{U}$ - $^{207}\text{Pb}/^{235}\text{U}$  concordia diagram.

## Acknowledgements

This project was financially supported by the Bureau of Minerals and Petroleum (BMP), Nuuk. The following people are acknowledged for involvement in analytical work and discussion of results: Ali Polat and Carlos Ordonez (University of Windsor), Dave Coller (EraMaptec), Matilde Rink Jørgensen, Rasmus Haugaard Nielsen, Louise Josefine Nielsen, Peter Venslev, Daniel Weilandt (University of Copenhagen), Peter Appel, Adam A. Garde, Carsten Guvad, Karen Merete Henriksen, Jørgen Kystol, Hanne Lamberts, Eric A. Nielsen, Agnete Steenfelt, Henrik Stendal, Bo Møller Stensgaard (GEUS).

## References

- Appel P.W.U., Garde A.A., Jørgensen M.S., Moberg E., Rasmussen T.M., Schjøth F. and Steenfelt A. 2003. Preliminary evaluation of the economic potential of the greenstone belts in the Nuuk region. Danmarks og Grønlands Geologiske Undersøgelse rapport 2003/94. 147 pp, 1 DVD.
- Chadwick B. and Coe K. 1988. Geological map of Greenland, 1:100 000, Ivisârtoq 64 V.2 Nord. Copenhagen: Geological Survey of Greenland.
- Friend C.R.L., Nutman A.P., Baadsgaard H., Kinny P.D. and McGregor V.R. 1996. Timing of late Archaean terrane assembly, crustal thickening and granite emplacement in the Nuuk region, southern West Greenland. *Earth and Planetary Science Letter*, 142: 353-365.
- Friend C.R.L. and Nutman A.P. 2005. New pieces to the Archaean terrane jigsaw puzzle in the Nuuk region, southern West Greenland: steps in transforming a simple insight into a complex regional tectonothermal model. *Journal of the Geological Society, London*, 162: 147-162.
- Garde A.A., Friend C.R.L., Nutman A.P. and Marker M. 2000. Rapid maturation and stabilisation of middle Archaean continental crust: the Akia terrane, southern West Greenland. *Bulletin of the Geological Society of Denmark*, 47: 1-27.
- Hollis, J.A., van Gool, J.A.M., Steenfelt, A. & Garde, A.A. 2004: Greenstone belts in the central Godthåbsfjord region, southern West Greenland. Danmarks og Grønlands Geologiske Undersøgelse Rapport 2004/110, 110 pp., 1 DVD.
- Hollis J.A. (ed.) 2005. Greenstone belts in the central Godthåbsfjord region, southern West Greenland: geochemistry, geochronology and petrography arising from 2004 field work, and digital map data. Danmarks og Grønlands Geologiske Undersøgelse Rapport 2005/42, 215pp.
- Hollis J.A., Schmid S., Stendal H., van Gool J.A.M., Weng W.L. 2006. Supracrustal belts in the Godthåbsfjord region, southern West Greenland: progress report on 2005 field work: geological mapping, regional hydrothermal alteration and tectonic sections. Danmarks og Grønlands Geologiske Undersøgelse Rapport 2006/7, 171 pp., 1 DVD.
- Jackson S.E., Pearson N.J., Griffin W.L., Belousova E.A. 2004. The application of laser ablation-inductively coupled plasma-mass spectrometry to in situ U-Pb zircon geochronology. *Chemical Geology*, 211: 47-69.
- Ludwig K.R. 2003. IsoPlot/Ex version 3.0: A geochronological toolkit for Microsoft Excel. Berkeley Geochronological Center, Berkeley.
- McGregor V.R. 1984. Geological map of Greenland, 1:100 000, Qôrquq 64 V.1 Syd. Copenhagen: Geological Survey of Greenland.
- Nielsen B.M., Rasmussen T.M. and Steenfelt A. 2004. Gold potential of the Nuuk region based on multi-parameter spatial modelling of known gold showings: interim report 2004. Danmarks og Grønlands Geologiske Undersøgelse Rapport 2004/121, 155 pp.
- Nutman, A.P., Friend, C.R.L., Baadsgaard, H. & McGregor, V.R. 1989: Evolution and assembly of Archean gneiss terranes in the Godthåbsfjord region, southern West Greenland: structural, metamorphic, and isotopic evidence. *Tectonics* 8, 573-589.
- Nutman A.P., McGregor V.R., Friend C.R.L., Bennett V.C. and Kinny P.D. 1996. The Itsaq gneiss complex of southern West Greenland; the world's most extensive record of early crustal evolution (3900–3600 Ma). *Precambrian Research* 78: 1-39.

- Nutman, A.P., Friend, C.R.L., Bennett, V.C. & McGregor, V.R. 2004a. Dating of the Ameralik dyke swarms of the Nuuk district, southern West Greenland: mafic intrusion events starting from c. 3510 Ma. *Journal of the Geological Society, London*, 161/3, 421-430.
- McGregor, V.R. 1984: Geological map of Greenland, 1:100 000, Qôrquq, sheet 64 V.1 Syd. Copenhagen: Grønlands Geologiske Undersøgelse.
- Stensgaard B.M., Steenfelt A. and Rasmussen T.M. 2005. Gold potential of the Nuuk region based on multi-parameter spatial modelling: progress 2005. Danmarks og Grønlands Geologiske Undersøgelse Rapport 2005/127, 207 pp.

## **Appendix 1: Tabulated LA-SF-ICPMS zircon U-Pb age data**

Zircon U-Pb age data were collected using a NewWave Research/Merchantek UP213 laser and Element2 sector-field inductively coupled plasma mass spectrometer at GEUS. Analysis numbers referred to images of zircon grains used to select analysis sites. Abbreviations are as follows: \* – analysis used in age calculation quoted in the text, Disc. – % discordance, gr – grain, hi U – high uranium, hom – homogeneous, osc – oscillatory zoned, pat – patchy, rho –  $^{235}\text{U}/^{207}\text{Pb}$ - $^{238}\text{U}/^{206}\text{Pb}$  error correlation, sec – sector, 204bdl – 204Pb was below the detection limit.

Analysis	sample	zircon morphology	$^{207}\text{Pb}$		U	Pb	$^{206}\text{Pb}$	Th	$^{207}\text{Pb}$	1 $\sigma$	$^{206}\text{Pb}^e$	1 $\sigma$	rho	$^{207}\text{Pb}$	1 $\sigma$	$^{207}\text{Pb}$	2 $\sigma$	$^{206}\text{Pb}$	2 $\sigma$	$^{207}\text{Pb}$	2 $\sigma$	Disc.
			(cps)	(ppm)	(ppm)		$^{204}\text{Pb}$	U	$^{235}\text{U}$	%	$^{238}\text{U}$	%		$^{206}\text{Pb}$	%	$^{235}\text{U}$	(Ma)	$^{238}\text{U}$	(Ma)	$^{206}\text{Pb}$	(Ma)	
64	496513	osc core	38290	51	30	1429	0.89	10.3462	2.0	0.4439	2.0	0.97	0.1690	0.5	2466	100	2368	93	2548	16	4.0	
79	496513	osc rim	683921	910	486	1410	0.67	10.8832	3.1	0.4521	3.0	0.97	0.1746	0.8	2513	155	2405	143	2602	25	4.3	
66	496513	osc core	294057	389	179	1329	0.22	10.4109	2.7	0.4093	2.7	0.99	0.1845	0.4	2472	134	2212	119	2693	12	10.5	
72	496513	hom core	153698	183	117	3029	0.68	13.5928	1.9	0.5327	1.8	0.97	0.1851	0.4	2722	103	2753	101	2699	15	-1.1	
86	496513	hom core	186458	223	142	8451	0.91	12.8923	1.8	0.5045	1.8	0.99	0.1853	0.3	2672	96	2633	94	2701	9	1.4	
74	496513	osc core	254837	297	168	2299	0.43	12.4302	1.8	0.4776	1.8	0.99	0.1888	0.3	2637	96	2517	91	2731	9	4.6	
80	496513	osc core	344253	411	264	1405	0.71	13.7736	2.0	0.5210	1.9	0.92	0.1917	0.8	2734	110	2704	101	2757	26	1.1	
59	496513	hom core	333776	312	200	1651	0.25	16.7267	3.1	0.5561	3.0	0.95	0.2182	1.0	2919	184	2850	170	2967	32	2.4	
67	496513	pat core	89101	81	62	2674	1.25	16.3855	2.2	0.5420	2.1	0.94	0.2193	0.8	2900	130	2792	117	2975	25	3.7	
73	496513	osc core	223041	197	138	994	0.54	16.8060	1.9	0.5551	1.8	0.98	0.2196	0.4	2924	110	2846	105	2978	13	2.7	
54	496513	pat core	58907	49	35	987	0.72	16.7107	2.0	0.5474	1.9	0.97	0.2214	0.5	2918	115	2814	108	2991	15	3.6	
75	496513	osc core	71697	62	46	2024	1.06	16.9420	2.0	0.5432	2.0	0.97	0.2262	0.5	2932	119	2797	110	3025	17	4.6	
77	496513	hom core	81959	65	49	171	0.42	18.4706	2.0	0.5864	1.9	0.92	0.2284	0.8	3015	122	2975	110	3041	26	1.3	
60	496513	osc core	218713	186	135	773	0.41	19.5188	1.9	0.5951	1.8	0.96	0.2379	0.5	3068	114	3010	107	3106	17	1.9	
78	496513	hom rim	54638	42	33	352	0.57	20.2966	1.9	0.6143	1.9	0.98	0.2396	0.4	3106	119	3087	116	3117	14	0.6	
55	496513	hom core	65311	48	38	484	0.83	19.3121	2.0	0.5776	1.8	0.91	0.2425	0.8	3058	124	2939	108	3136	27	3.9	
93	496516	osc rim	87357	111	55	3818	0.05	11.7137	1.9	0.4766	1.8	0.98	0.1783	0.4	2582	96	2512	92	2637	12	2.7	
100	496516	hom rim	36609	37	21	764	0.36	13.5950	2.2	0.4894	2.1	0.94	0.2015	0.8	2722	119	2568	106	2838	25	5.6	
103	496516	osc core	51007	49	31	1256	0.43	15.8687	1.9	0.5297	1.9	0.97	0.2173	0.5	2869	111	2740	103	2961	15	4.5	
104	496516	osc core	45676	40	27	1803	0.43	17.0623	2.1	0.5617	2.0	0.94	0.2203	0.7	2938	122	2873	112	2983	22	2.2	
111	496516	osc core	57450	50	35	1669	0.58	18.0069	2.1	0.5925	1.9	0.90	0.2204	0.9	2990	129	3000	117	2984	30	-0.3	
117	496516	sec core	62197	53	34	2164	0.34	16.7720	1.9	0.5457	1.8	0.98	0.2229	0.4	2922	108	2807	102	3002	13	3.9	
102	496516	hom rim	69938	62	38	1608	0.22	16.9425	2.0	0.5489	1.9	0.97	0.2239	0.5	2932	117	2820	109	3009	15	3.8	
94	496516	osc core	70199	60	42	1849	0.61	17.0575	1.8	0.5515	1.8	0.98	0.2243	0.4	2938	106	2831	100	3012	12	3.6	
115	496516	hom rim	113378	96	61	3705	0.09	17.9275	1.8	0.5780	1.8	0.99	0.2250	0.3	2986	109	2940	106	3017	9	1.5	

Analysis	sample	zircon morphology	<sup>207</sup> Pb			U	Pb	<sup>206</sup> Pb	Th	<sup>207</sup> Pb	1 σ	<sup>206</sup> Pb <sup>e</sup>	1 σ	rho	<sup>207</sup> Pb	1 σ	<sup>207</sup> Pb	2 σ	<sup>206</sup> Pb	2 σ	<sup>207</sup> Pb	2 σ
			(cps)	(ppm)	(ppm)	<sup>204</sup> Pb	U	<sup>235</sup> U	%	<sup>238</sup> U	%	<sup>206</sup> Pb	%	<sup>235</sup> U	(Ma)	<sup>238</sup> U	(Ma)	<sup>206</sup> Pb	(Ma)	<sup>207</sup> Pb	(Ma)	
*99	496516	osc core	95551	85	57	2401	0.61	16.6803	1.9	0.5350	1.9	0.98	0.2261	0.3	2917	112	2762	105	3025	11	5.3	
*90	496516	osc core	86371	75	52	1813	0.57	17.2324	1.9	0.5526	1.8	0.98	0.2262	0.3	2948	109	2836	103	3025	11	3.8	
*105	496516	osc core	41469	35	24	1243	0.52	17.8395	2.1	0.5703	2.1	0.97	0.2269	0.5	2981	127	2909	120	3030	18	2.4	
*113	496516	osc core	35891	29	23	1198	0.74	19.4650	1.8	0.6211	1.8	0.96	0.2273	0.5	3065	113	3114	110	3033	16	-1.6	
*114	496516	osc core	72207	61	41	1829	0.52	17.1537	1.9	0.5463	1.8	0.97	0.2277	0.4	2943	110	2810	102	3036	14	4.5	
*101	496516	osc core	77599	66	45	2054	0.53	17.6742	2.1	0.5625	2.0	0.97	0.2279	0.5	2972	123	2877	115	3037	16	3.2	
*112	496516	osc core	61271	52	36	1539	0.45	18.0054	1.9	0.5716	1.9	0.97	0.2285	0.4	2990	116	2914	110	3041	14	2.5	
*88	496516	osc core	87004	72	48	2573	0.56	16.9600	2.0	0.5366	2.0	0.99	0.2292	0.3	2933	118	2769	110	3047	11	5.6	
*107	496516	osc core	74367	62	44	2504	0.54	18.1587	1.9	0.5740	1.8	0.98	0.2294	0.3	2998	111	2924	107	3048	10	2.5	
*92	496516	osc core	39074	32	21	1159	0.46	17.8243	1.9	0.5633	1.8	0.96	0.2295	0.5	2980	113	2880	105	3049	16	3.4	
*116	496516	osc core	84415	70	51	2334	0.52	19.0035	2.0	0.6002	2.0	0.98	0.2296	0.4	3042	121	3030	118	3050	11	0.4	
*91	496516	osc core	116864	100	71	2651	0.71	17.4677	1.9	0.5508	1.8	0.98	0.2300	0.3	2961	111	2828	104	3052	11	4.5	
*106	496516	osc core	55234	47	31	2045	0.47	17.5004	1.8	0.5513	1.8	0.97	0.2302	0.4	2963	109	2830	102	3054	13	4.5	
*89	496516	osc core	83757	70	52	2615	0.86	17.7380	1.9	0.5577	1.8	0.98	0.2307	0.4	2976	111	2857	104	3057	12	4.0	
*98	496516	sec core	20813	16	11	886	0.70	18.0271	2.0	0.5666	1.9	0.96	0.2308	0.6	2991	118	2894	109	3057	18	3.3	
*87	496516	osc core	70937	58	41	1951	0.58	17.8802	1.9	0.5610	1.8	0.98	0.2312	0.4	2983	111	2871	104	3060	13	3.8	
*8	496519	hom gr	1039106	1307	576	10159	0.09	10.7064	4.0	0.4270	4.0	0.98	0.1818	0.8	2498	201	2292	181	2670	25	8.2	
15	496519	hom core	104851	113	60	2798	0.36	12.2620	2.6	0.4438	2.5	0.97	0.2004	0.6	2625	134	2368	117	2829	21	9.8	
21	496519	osc core	223952	221	151	1211	0.85	16.0058	2.6	0.5768	2.5	0.97	0.2013	0.6	2877	147	2936	146	2836	19	-2.0	
9	496519	osc core	85290	90	49	4097	0.32	13.3114	2.0	0.4724	1.8	0.89	0.2044	0.9	2702	109	2494	90	2861	30	7.7	
16	496519	osc core	58572	58	36	1462	0.74	14.2516	2.0	0.5049	1.9	0.96	0.2047	0.6	2767	110	2635	101	2864	18	4.8	
20	496519	hom rim	43681	39	26	941	0.66	15.2871	1.9	0.5413	1.8	0.97	0.2048	0.5	2833	107	2789	102	2865	16	1.6	
11	496519	osc core	55948	27	23	699	0.31	30.4130	2.1	0.6976	1.9	0.91	0.3162	0.8	3500	146	3411	130	3551	26	2.5	
10	496519	hom rim	11556	6	7	144		36.9828	65.8	0.7892	13.3	0.20	0.3399	64.4	3693	4857	3750	996	3662	1968	-1.5	
25	498420	pat gr	503323	1752	509	1137	0.40	6.5360	3.7	0.2617	3.6	0.99	0.1812	0.6	2051	151	1498	109	2663	21	26.9	

Analysis	sample	morphology	zircon		$^{207}\text{Pb}$	U	Pb	$^{206}\text{Pb}$	Th	$^{207}\text{Pb}$	1 $\sigma$	$^{206}\text{Pb}^e$	1 $\sigma$	rho	$^{207}\text{Pb}$	1 $\sigma$	$^{207}\text{Pb}$	2 $\sigma$	$^{206}\text{Pb}$	2 $\sigma$	$^{207}\text{Pb}$	2 $\sigma$	Disc.
			(cps)	(ppm)	(ppm)	$^{204}\text{Pb}$	U	$^{235}\text{U}$	%	$^{238}\text{U}$	%	$^{206}\text{Pb}$	%	$^{235}\text{U}$	(Ma)	$^{238}\text{U}$	(Ma)	$^{206}\text{Pb}$	(Ma)				
21	498420	hom core	279295	532	245	980	0.27	10.5678	4.4	0.4092	4.3	0.98	0.1873	0.8	2486	219	2211	191	2719	28	11.0		
10	498420	hom core	236801	380	219	23833	0.42	13.5434	3.4	0.5103	3.4	0.99	0.1925	0.4	2718	184	2658	179	2764	12	2.2		
26	498420	hom core	113749	177	113	11958	0.42	15.2481	3.5	0.5741	3.4	0.99	0.1926	0.4	2831	196	2924	201	2765	14	-3.3		
14	498420	hom core	182813	290	163	8991	0.31	13.4652	4.0	0.5066	4.0	0.99	0.1928	0.4	2713	218	2642	211	2766	14	2.6		
7	498420	hom core	130769	209	157	24093	0.73	17.3673	3.3	0.6476	3.3	0.99	0.1945	0.4	2955	197	3219	213	2781	14	-8.9		
24	498420	hom core	149550	217	147	1111	1.06	14.5344	3.7	0.5405	3.6	0.99	0.1950	0.6	2785	206	2785	203	2785	21	0.0		
15	498420	hom core	251912	412	232	4801	0.30	13.8171	4.2	0.5131	4.1	0.97	0.1953	1.0	2737	228	2670	217	2787	32	2.5		
11	498420	hom core	135532	211	130	1209	0.72	13.6527	3.4	0.5055	3.3	0.99	0.1959	0.4	2726	184	2637	176	2792	13	3.2		
8	498420	hom core	141286	220	137	5900	0.56	14.6647	3.3	0.5425	3.3	0.99	0.1961	0.4	2794	187	2794	186	2794	12	0.0		
13	498420	hom core	131603	215	129	2947	0.56	14.2911	3.5	0.5279	3.4	0.97	0.1963	0.9	2769	196	2733	188	2796	29	1.3		
23	498420	hom core	95739	171	102	1821	0.54	14.3563	3.5	0.5233	3.4	0.98	0.1990	0.7	2774	192	2713	185	2818	22	2.2		
27	498420	pat gr	282841	471	247	1131	0.53	11.6905	3.6	0.4254	3.6	0.99	0.1993	0.6	2580	187	2285	163	2820	19	11.4		
33	498420	pat gr	156805	381	227	2689	0.49	14.9307	3.3	0.5383	3.3	0.99	0.2012	0.4	2811	187	2776	183	2836	14	1.2		
9	498420	hom core	202764	339	213	725	0.83	13.8846	4.2	0.4929	4.1	0.97	0.2043	1.1	2742	230	2583	209	2861	35	5.8		
20	498420	hom core	40250	85	35	536	0.94	8.0606	4.0	0.2852	4.0	0.98	0.2050	0.7	2238	181	1618	129	2866	23	27.7		
16	498420	hom core	99390	153	105	852	1.23	14.9346	3.6	0.5282	3.5	0.97	0.2051	0.8	2811	202	2734	191	2867	27	2.8		
22	498420	hom core	157568	274	116	626	0.28	9.9122	3.8	0.3431	3.6	0.96	0.2095	1.1	2427	184	1902	138	2902	36	21.6		
12	498420	hom core	80621	263	59	481	2.71	5.3175	4.3	0.1773	4.3	0.99	0.2176	0.7	1872	163	1052	90	2963	21	43.8		
94	498422	hom gr	458761	641	321	480397	0.02	11.5735	2.3	0.4913	2.3	0.99	0.1709	0.3	2571	120	2576	119	2566	9	-0.2		
91	498422	hom gr	541084	749	389	204bdl	0.04	12.0520	2.5	0.5076	2.3	0.93	0.1722	1.0	2608	132	2646	124	2579	32	-1.4		
*98	498422	hom gr	287674	369	190	131115	0.03	12.0621	2.6	0.5035	2.6	0.99	0.1737	0.3	2609	137	2629	137	2594	9	-0.8		
*93	498422	hom gr	292248	406	161	23473	0.06	9.2120	3.0	0.3842	2.9	0.98	0.1739	0.6	2359	141	2096	123	2596	19	11.2		
*90	498422	hom gr	281052	395	197	66509	0.11	11.6250	2.5	0.4838	2.5	0.99	0.1743	0.3	2575	127	2544	125	2599	9	1.2		
*92	498422	hom gr	205037	260	127	204bdl	0.11	11.3500	2.5	0.4703	2.5	0.99	0.1751	0.4	2552	127	2485	122	2607	14	2.7		
152	498447	hom core	124779	251	115	5781	0.08	10.4373	3.4	0.4390	3.4	0.99	0.1724	0.3	2474	167	2346	157	2581	11	5.2		

Analysis	sample	morphology	zircon		$^{207}\text{Pb}$	U	Pb	$^{206}\text{Pb}$	Th	$^{207}\text{Pb}$	1 $\sigma$	$^{206}\text{Pb}^e$	1 $\sigma$	rho	$^{207}\text{Pb}$	1 $\sigma$	$^{207}\text{Pb}$	2 $\sigma$	$^{206}\text{Pb}$	2 $\sigma$	$^{207}\text{Pb}$	2 $\sigma$	Disc.
			(cps)	(ppm)	(ppm)	$^{204}\text{Pb}$	U	$^{235}\text{U}$	%	$^{238}\text{U}$	%	$^{206}\text{Pb}$	%	$^{235}\text{U}$	(Ma)	$^{238}\text{U}$	(Ma)	$^{206}\text{Pb}$	(Ma)				
*179	498447	hom core	71935	126	61	9074	0.06	11.2454	3.4	0.4656	3.4	0.99	0.1752	0.4	2544	173	2464	166	2608	15	3.1		
*176	498447	hom core	94450	165	82	7044	0.10	11.5092	3.3	0.4763	3.3	1.00	0.1752	0.3	2565	172	2511	167	2608	11	2.1		
*168	498447	hom core	121241	232	110	35836	0.14	10.8434	3.4	0.4486	3.4	1.00	0.1753	0.3	2510	169	2389	160	2609	10	4.8		
*157	498447	hom core	102171	183	85	7026	0.07	10.7535	3.4	0.4445	3.4	1.00	0.1754	0.3	2502	169	2371	160	2610	10	5.2		
*155	498447	hom core	94967	173	80	8161	0.09	10.6737	3.5	0.4406	3.5	0.99	0.1757	0.4	2495	175	2354	164	2613	14	5.7		
*150	498447	hom core	97706	171	85	9225	0.08	11.6158	3.4	0.4794	3.4	1.00	0.1757	0.3	2574	175	2525	171	2613	11	1.9		
*156	498447	hom core	102989	193	96	13368	0.15	11.4020	3.4	0.4706	3.4	1.00	0.1757	0.3	2557	173	2486	168	2613	10	2.8		
*163	498447	hom core	87386	146	74	6351	0.12	11.7006	3.4	0.4818	3.4	0.99	0.1761	0.4	2581	174	2535	170	2617	13	1.8		
*180	498447	hom core	94782	159	85	5480	0.09	12.5246	3.3	0.5149	3.3	1.00	0.1764	0.3	2645	177	2678	178	2619	11	-1.2		
*172	498447	hom rim	49461	84	47	1784	0.16	12.9704	3.5	0.5332	3.5	0.99	0.1764	0.6	2678	190	2755	193	2620	20	-2.9		
*159	498447	hom core	71726	118	64	3461	0.08	12.5324	3.4	0.5150	3.4	0.99	0.1765	0.4	2645	182	2678	183	2620	14	-1.2		
*182	498447	hom core	46644	79	42	3333	0.08	12.5064	3.5	0.5137	3.4	0.98	0.1766	0.7	2643	184	2672	183	2621	22	-1.1		
181	498447	hom core	76593	135	70	3450	0.18	11.9096	3.4	0.4840	3.4	0.99	0.1785	0.4	2597	176	2545	171	2639	14	2.0		
177	498447	hom core	73348	119	59	4686	0.12	11.6037	3.4	0.4680	3.3	0.99	0.1798	0.4	2573	173	2475	166	2651	13	3.8		
144	498447	hom core	95802	161	78	1582	0.18	11.2744	3.9	0.4493	3.9	0.99	0.1820	0.5	2546	198	2392	184	2671	18	6.1		
178	498447	osc core	67012	114	57	1869	0.25	11.8603	3.5	0.4626	3.5	0.99	0.1859	0.4	2593	181	2451	170	2707	14	5.5		
153	498447	osc core	143858	237	139	832	0.52	13.1980	3.4	0.4869	3.4	0.98	0.1966	0.7	2694	186	2557	173	2798	22	5.1		
154	498447	osc core	98762	165	97	597	0.98	12.6097	3.8	0.4648	3.5	0.92	0.1968	1.5	2651	202	2461	172	2800	50	7.2		
167	498447	osc core	74034	99	62	11507	0.44	15.4555	3.7	0.5237	3.5	0.96	0.2140	1.0	2844	210	2715	192	2936	34	4.5		
68	498452	hom rim	212089	330	201	204bdl	0.33	14.8205	7.5	0.5504	7.4	0.99	0.1953	0.8	2804	419	2827	420	2787	26	-0.8		
64	498452	osc core	102347	132	83	204bdl	0.32	16.7080	3.2	0.5423	3.2	0.99	0.2235	0.4	2918	188	2793	179	3006	13	4.3		
61	498452	osc core	52219	73	43	204bdl	0.46	15.1256	3.3	0.4899	3.3	0.99	0.2239	0.5	2823	187	2570	169	3009	17	9.0		
69	498452	osc core	122668	171	98	123200	0.40	14.9850	3.3	0.4852	3.2	0.99	0.2240	0.4	2814	184	2550	165	3010	13	9.4		
47	498452	osc core	79305	108	74	1335	0.91	16.8677	3.2	0.5459	3.2	0.99	0.2241	0.4	2927	188	2808	179	3010	14	4.1		
75	498452	osc core	89959	128	77	204bdl	0.42	15.5590	3.2	0.5035	3.2	0.99	0.2241	0.4	2850	185	2629	169	3011	14	7.8		

Analysis	sample	zircon morphology	<sup>207</sup> Pb	U	Pb	<sup>206</sup> Pb	Th	<sup>207</sup> Pb	1 σ	<sup>206</sup> Pb <sup>e</sup>	1 σ	rho	<sup>207</sup> Pb	1 σ	<sup>207</sup> Pb	2 σ	<sup>206</sup> Pb	2 σ	<sup>207</sup> Pb	2 σ	Disc.
			(cps)	(ppm)	(ppm)	<sup>204</sup> Pb	U	<sup>235</sup> U	%	<sup>238</sup> U	%	<sup>206</sup> Pb	%	<sup>235</sup> U	(Ma)	<sup>238</sup> U	(Ma)	<sup>206</sup> Pb	(Ma)		
77	498452	osc rim	287130	369	239	597	0.52	16.5680	3.3	0.5351	3.2	0.96	0.2246	0.9	2910	191	2763	174	3014	28	5.1
73	498452	osc core	60634	85	58	204bdl	0.60	17.2833	3.3	0.5580	3.2	0.99	0.2246	0.4	2951	193	2859	185	3014	13	3.1
65	498452	osc core	52549	64	39	539	0.69	14.9285	3.5	0.4797	3.4	0.97	0.2257	0.8	2811	198	2526	173	3022	26	10.1
51	498452	osc core	63754	90	54	3859	0.56	15.1194	3.2	0.4845	3.2	0.99	0.2263	0.5	2823	183	2547	164	3026	15	9.8
46	498452	osc core	84096	114	75	8026	0.37	17.7882	3.2	0.5666	3.2	0.99	0.2277	0.4	2978	192	2894	185	3036	12	2.8
50	498452	osc core	36447	38	35	204bdl	0.44	25.2483	8.1	0.8006	8.0	0.99	0.2287	0.9	3318	537	3791	610	3043	30	-14.3
52	498452	osc core	48162	67	44	204bdl	0.60	16.5906	3.3	0.5217	3.2	0.97	0.2306	0.8	2911	195	2707	176	3056	25	7.0
63	498452	hom core	143230	198	121	1433	0.41	16.6210	3.3	0.5217	3.3	0.98	0.2311	0.6	2913	193	2706	176	3059	19	7.1
79	498452	osc core	68875	96	63	6025	0.62	17.2409	3.3	0.5386	3.2	0.99	0.2322	0.5	2948	192	2778	178	3067	17	5.8
60	498452	osc core	127907	179	116	3128	0.45	17.3369	3.2	0.5401	3.2	0.99	0.2328	0.4	2954	191	2784	178	3071	14	5.7
62	498452	hom core	234420	327	196	1956	0.29	16.4464	3.2	0.5105	3.2	0.98	0.2336	0.6	2903	188	2659	169	3077	20	8.4
66	498452	osc core	143450	192	110	754	0.38	15.5274	3.3	0.4705	3.2	0.98	0.2393	0.6	2848	188	2486	161	3116	20	12.7
72	498452	osc core	128926	150	107	404	1.20	19.2594	3.8	0.5743	3.4	0.88	0.2432	1.8	3055	233	2925	197	3141	57	4.2
80	498452	osc core	89603	112	67	686	0.45	16.7801	3.9	0.4704	3.8	0.97	0.2587	0.9	2922	226	2485	187	3239	30	15.0
49	498452	osc core	243902	300	183	592	0.34	18.3711	3.5	0.5088	3.3	0.94	0.2619	1.2	3009	209	2652	173	3258	37	11.9
81	498452	osc core	128685	123	89	555	0.65	21.7156	3.6	0.5714	3.3	0.91	0.2756	1.4	3171	226	2914	190	3338	45	8.1
34	498481	osc core	45768	65	39	8198	0.39	14.4403	3.4	0.5296	3.3	0.99	0.1978	0.4	2779	187	2740	183	2808	14	1.4
*35	498481	hom core	271242	353	280	3402	1.68	16.4453	3.5	0.5615	3.4	0.99	0.2124	0.4	2903	202	2873	198	2924	15	1.0
*37	498481	osc core	280908	366	244	6147	0.48	16.8981	3.3	0.5758	3.3	0.99	0.2128	0.4	2929	196	2932	194	2927	14	-0.1
*38	498481	osc core	211535	270	208	3268	1.50	16.0043	3.4	0.5450	3.4	0.99	0.2130	0.4	2877	198	2804	192	2928	11	2.5
*36	498481	hom core	363099	469	397	3974	1.62	16.1717	3.3	0.5481	3.3	1.00	0.2140	0.2	2887	192	2817	187	2936	8	2.4
*39	498481	hom core	213934	265	207	70687	1.36	17.2231	3.3	0.5785	3.3	1.00	0.2159	0.3	2947	196	2943	195	2950	10	0.2
286	498496	hom core	612349	1183	745	982	0.59	13.1226	3.8	0.5167	3.3	0.89	0.1842	1.7	2689	202	2685	179	2691	58	0.1
270	498496	hom core	79955	145	84	1195	0.58	12.2806	7.2	0.4769	7.1	0.99	0.1868	1.2	2626	377	2514	356	2714	41	4.3
269	498496	hom core	74356	103	71	723	0.26	16.3171	4.1	0.6238	4.1	0.98	0.1897	0.8	2896	240	3125	254	2740	25	-7.9

Analysis	sample	morphology	zircon		$^{207}\text{Pb}$	U	Pb	$^{206}\text{Pb}$	Th	$^{207}\text{Pb}$	1 σ	$^{206}\text{Pb}^e$	1 σ	rho	$^{207}\text{Pb}$	1 σ	$^{207}\text{Pb}$	2 σ	$^{206}\text{Pb}$	2 σ	$^{207}\text{Pb}$	2 σ	Disc.
			(cps)	(ppm)	(ppm)	$^{204}\text{Pb}$	U	$^{235}\text{U}$	%	$^{238}\text{U}$	%	$^{206}\text{Pb}$	%	$^{235}\text{U}$	(Ma)	$^{238}\text{U}$	(Ma)	$^{206}\text{Pb}$	(Ma)	$^{207}\text{Pb}$	(Ma)		
285	498496	hom core	340388	569	342	10347	0.53	13.4489	3.4	0.5090	3.4	0.98	0.1916	0.6	2712	186	2652	179	2756	20	2.2		
262	498496	hom core	133088	180	113	1182	0.36	14.3530	3.5	0.5429	3.4	0.98	0.1918	0.7	2773	194	2795	192	2757	23	-0.8		
280	498496	osc core	156517	250	135	6975	0.12	13.4277	3.3	0.5046	3.3	1.00	0.1930	0.3	2710	181	2634	176	2768	9	2.8		
297	498496	hom core	287731	502	264	1233	0.19	12.6356	4.0	0.4711	3.9	0.99	0.1945	0.7	2653	211	2488	195	2781	22	6.2		
273	498496	hom core	60051	80	55	970	0.50	15.3827	3.7	0.5703	3.7	0.99	0.1956	0.6	2839	210	2909	213	2790	19	-2.5		
261	498496	hom core	219481	322	219	534	0.34	16.8310	4.0	0.5913	3.6	0.91	0.2064	1.7	2925	235	2995	218	2878	55	-2.4		
284	498496	hom core	96832	106	74	325	0.20	16.8953	4.6	0.5630	3.6	0.78	0.2177	2.9	2929	272	2879	208	2963	95	1.7		
276	498496	hom rim	49669	65	45	12881	0.91	15.7018	3.5	0.5214	3.5	0.99	0.2184	0.5	2859	201	2705	188	2969	15	5.4		
86	498497	hom core	280182	528	252	2470	0.09	10.9043	3.7	0.4553	3.6	0.98	0.1737	0.7	2515	185	2419	175	2593	22	3.8		
85	498497	pat core	468900	902	409	909	0.05	10.4374	3.6	0.4270	3.5	0.96	0.1773	1.0	2474	180	2292	161	2628	32	7.4		
102	498497	hom rim	387533	726	370	29887	0.09	12.0487	3.5	0.4901	3.5	0.99	0.1783	0.5	2608	184	2571	179	2637	18	1.4		
79	498497	osc core	469268	840	434	3494	0.13	12.0630	3.4	0.4889	3.4	0.99	0.1790	0.6	2609	179	2566	174	2643	18	1.7		
101	498497	hom core	548771	685	401	135	0.37	11.6283	3.6	0.4701	3.5	0.98	0.1794	0.6	2575	183	2484	174	2647	21	3.5		
92	498497	hom core	603889	1025	515	592	0.25	11.4199	3.5	0.4612	3.4	0.97	0.1796	0.9	2558	178	2445	165	2649	30	4.4		
87	498497	hom core	326941	660	286	2946	0.09	10.1669	3.7	0.4099	3.4	0.90	0.1799	1.6	2450	184	2214	149	2652	54	9.6		
91	498497	hom core	673568	1215	601	38951	0.02	12.0967	3.5	0.4805	3.4	0.98	0.1826	0.7	2612	183	2529	174	2676	22	3.2		
104	498497	pat core	516270	1017	436	752	0.04	10.3486	3.7	0.4005	3.5	0.93	0.1874	1.4	2466	184	2171	151	2720	45	12.0		
98	498497	hom rim	380243	582	323	429	0.13	13.0469	3.5	0.5040	3.3	0.94	0.1878	1.2	2683	190	2631	175	2723	40	1.9		
103	498497	hom core	221663	310	165	348	0.16	12.3231	3.5	0.4689	3.4	0.96	0.1906	0.9	2629	184	2479	167	2747	31	5.7		
100	498497	osc core	619719	1753	496	883	0.03	6.9300	5.7	0.2629	4.7	0.82	0.1912	3.3	2103	242	1505	142	2752	108	28.4		
90	498497	hom rim	153293	221	126	1048	0.13	13.8844	3.4	0.5228	3.4	0.98	0.1926	0.7	2742	188	2711	182	2765	23	1.1		
183	498762	pat core	281739	501	241	2964	0.09	11.7315	3.6	0.4578	3.4	0.94	0.1859	1.2	2583	188	2430	166	2706	41	5.9		
211	498762	osc core	193693	331	121	1471	0.11	9.0466	6.6	0.3335	6.3	0.95	0.1967	2.1	2343	311	1855	234	2799	68	20.8		
216	498762	osc core	329867	423	249	3409	0.06	16.1025	3.8	0.5496	3.8	1.00	0.2125	0.2	2883	222	2823	217	2925	7	2.1		
204	498762	osc core	249008	303	184	1704	0.04	16.8325	3.7	0.5599	3.7	0.99	0.2180	0.5	2925	216	2866	209	2966	16	2.0		

Analysis	sample	morphology	zircon		$^{207}\text{Pb}$	U	Pb	$^{206}\text{Pb}$	Th	$^{207}\text{Pb}$	1 $\sigma$	$^{206}\text{Pb}^e$	1 $\sigma$	rho	$^{207}\text{Pb}$	1 $\sigma$	$^{207}\text{Pb}$	2 $\sigma$	$^{206}\text{Pb}$	2 $\sigma$	$^{207}\text{Pb}$	2 $\sigma$	Disc.
			(cps)	(ppm)	(ppm)	$^{204}\text{Pb}$	U	$^{235}\text{U}$	%	$^{238}\text{U}$	%	$^{206}\text{Pb}$	%	$^{235}\text{U}$	(Ma)	$^{238}\text{U}$	(Ma)	$^{206}\text{Pb}$	(Ma)	$^{207}\text{Pb}$	(Ma)		
197	498762	osc core	179139	214	133	1429	0.13	17.1596	3.7	0.5700	3.6	0.98	0.2184	0.8	2944	217	2908	209	2969	25	1.2		
184	498762	hom rim	73530	83	57	1193	0.18	19.0418	3.4	0.6281	3.3	0.99	0.2199	0.4	3044	206	3142	211	2980	14	-3.2		
220	498762	osc core	78300	84	65	1590	0.09	21.7305	3.6	0.7103	3.4	0.94	0.2219	1.3	3172	230	3460	234	2994	41	-9.1		
215	498762	osc core	151673	182	109	1565	0.07	17.0483	3.6	0.5482	3.5	0.98	0.2255	0.6	2938	209	2818	198	3021	20	4.1		
206	498762	osc core	11372	13	11	879	0.45	23.7238	4.3	0.7613	3.4	0.80	0.2260	2.6	3257	280	3649	251	3024	83	-12.0		
221	498762	osc core	63204	76	48	15975	0.40	16.4898	3.7	0.5290	3.7	0.99	0.2261	0.4	2906	214	2737	200	3025	13	5.8		
210	498762	osc core	208275	249	171	2449	0.13	19.5419	3.3	0.6266	3.3	0.99	0.2262	0.3	3069	203	3136	207	3025	11	-2.2		
217	498762	osc core	77847	89	61	699	0.20	18.6520	4.0	0.5976	3.9	0.98	0.2264	0.7	3024	242	3020	238	3027	22	0.1		
209	498762	osc core	97529	103	71	1007	0.29	19.7448	3.5	0.6322	3.4	0.98	0.2265	0.7	3079	214	3158	215	3028	24	-2.6		
207	498762	osc rim	7502	8	6	1449	0.18	20.9610	3.9	0.6711	3.7	0.95	0.2265	1.2	3137	242	3310	243	3028	38	-5.5		
194	498762	osc core	80507	84	64	2840	0.31	20.8217	3.4	0.6666	3.4	0.99	0.2265	0.3	3130	211	3293	221	3028	11	-5.2		
219	498762	hom core	9081	9	6	6908	0.06	20.0616	5.2	0.6369	5.0	0.96	0.2285	1.4	3094	319	3177	315	3041	45	-2.7		
189	498762	pat core	169962	193	122	679	0.13	17.7985	3.8	0.5606	3.5	0.93	0.2303	1.4	2979	226	2869	201	3054	45	3.7		
218	498762	osc core	43576	49	33	587	0.27	18.5648	3.7	0.5769	3.5	0.95	0.2334	1.2	3019	222	2936	205	3075	38	2.8		
205	498762	osc rim	118013	129	85	598	0.07	18.9494	3.5	0.5825	3.5	0.98	0.2359	0.6	3039	213	2959	204	3093	20	2.6		
203	498762	osc core	84048	99	65	551	0.23	18.5907	3.6	0.5650	3.4	0.97	0.2387	0.9	3021	215	2887	199	3111	28	4.4		
191	498762	osc core	148760	153	102	530	0.23	18.9830	3.7	0.5713	3.4	0.92	0.2410	1.4	3041	224	2913	198	3127	45	4.2		
190	498762	osc core	60049	63	45	572	0.38	20.0091	3.8	0.5994	3.5	0.91	0.2421	1.6	3092	237	3028	210	3134	52	2.1		
198	498762	osc core	136560	134	88	374	0.25	18.4542	3.8	0.5455	3.6	0.97	0.2454	1.0	3014	227	2806	204	3155	31	6.9		
192	498762	osc core	90883	99	53	259	0.12	14.6559	5.0	0.4226	4.8	0.96	0.2515	1.3	2793	278	2272	217	3194	42	18.6		
*61	498803	hom core	343644	756	529	24175	0.95	9.2014	3.5	0.3936	3.5	0.99	0.1695	0.5	2358	165	2140	149	2553	15	9.3		
74	498803	hom core	438753	1034	571	199479	0.79	8.9455	3.5	0.3803	3.5	1.00	0.1706	0.2	2332	164	2078	146	2563	7	10.9		
*52	498803	hom core	520038	1088	656	8638	0.98	9.4377	3.5	0.4004	3.4	0.99	0.1710	0.5	2382	166	2171	149	2567	17	8.8		
*55	498803	hom core	581419	1302	676	399532	0.48	9.2271	3.4	0.3913	3.4	1.00	0.1710	0.3	2361	162	2129	145	2568	10	9.8		
*67	498803	hom core	399486	923	622	62065	1.04	9.5409	3.4	0.4037	3.4	1.00	0.1714	0.2	2391	161	2186	146	2572	8	8.6		

Analysis	sample	morphology	zircon		$^{207}\text{Pb}$	U	Pb	$^{206}\text{Pb}$	Th	$^{207}\text{Pb}$	1 $\sigma$	$^{206}\text{Pb}^e$	1 $\sigma$	rho	$^{207}\text{Pb}$	1 $\sigma$	$^{207}\text{Pb}$	2 $\sigma$	$^{206}\text{Pb}$	2 $\sigma$	$^{207}\text{Pb}$	2 $\sigma$	Disc.
			(cps)	(ppm)	(ppm)	$^{204}\text{Pb}$	U	$^{235}\text{U}$	%	$^{238}\text{U}$	%	$^{206}\text{Pb}$	%	$^{235}\text{U}$	(Ma)	$^{238}\text{U}$	(Ma)	$^{206}\text{Pb}$	(Ma)				
*40	498803	hom core	409069	876	591	156708	1.40	10.3586	3.4	0.4382	3.3	0.99	0.1714	0.6	2467	168	2343	157	2572	19	5.1		
*78	498803	hom core	324321	748	504	19164	1.41	9.8184	3.4	0.4146	3.3	0.99	0.1717	0.4	2418	162	2236	149	2575	15	7.5		
77	498803	hom core	382889	861	540	44186	1.27	9.0004	3.5	0.3798	3.5	0.99	0.1719	0.4	2338	165	2076	146	2576	13	11.2		
63	498803	hom core	504676	1148	705	204bdl	0.73	9.2258	3.5	0.3892	3.5	1.00	0.1719	0.3	2361	167	2119	149	2577	10	10.2		
*51	498803	hom core	468050	967	596	1257	1.07	10.0892	3.5	0.4254	3.4	0.97	0.1720	0.9	2443	170	2285	154	2577	29	6.5		
*68	498803	hom core	380232	800	470	31579	1.15	9.8587	3.3	0.4155	3.3	0.99	0.1721	0.5	2422	161	2240	148	2578	15	7.5		
*53	498803	hom core	396720	887	604	53580	1.20	9.7542	3.4	0.4110	3.3	1.00	0.1721	0.3	2412	162	2219	148	2579	9	8.0		
62	498803	hom core	424326	978	581	20227	0.65	9.1486	3.5	0.3854	3.5	1.00	0.1722	0.3	2353	163	2101	145	2579	10	10.7		
76	498803	hom core	280366	612	462	15463	1.44	9.2759	3.7	0.3902	3.6	0.99	0.1724	0.5	2366	174	2124	155	2581	17	10.2		
*46	498803	hom core	486131	1047	617	204bdl	0.91	9.5454	3.4	0.4014	3.4	0.99	0.1725	0.4	2392	165	2175	148	2582	15	9.1		
72	498803	hom core	359414	837	494	176409	0.95	8.8964	3.5	0.3740	3.5	1.00	0.1725	0.3	2327	163	2048	143	2582	9	12.0		
59	498803	hom core	352064	794	486	94239	1.00	8.9649	3.5	0.3764	3.5	1.00	0.1727	0.2	2334	164	2059	144	2584	8	11.8		
*48	498803	hom core	536686	1167	643	96842	0.44	9.6654	4.4	0.4054	4.3	1.00	0.1729	0.4	2403	209	2194	190	2586	13	8.7		
73	498803	hom core	625377	1425	782	92165	0.49	9.2824	4.0	0.3893	4.0	0.99	0.1729	0.5	2366	189	2120	168	2586	17	10.4		
*42	498803	hom core	347603	729	587	26320	1.45	10.0332	3.6	0.4197	3.4	0.95	0.1734	1.2	2438	177	2259	155	2590	40	7.3		
66	498803	hom core	411621	901	584	6215	1.15	9.1173	4.5	0.3804	4.4	0.97	0.1738	1.2	2350	213	2078	182	2595	39	11.6		
60	498803	hom core	342964	757	480	38108	0.95	9.3202	4.0	0.3867	3.9	0.99	0.1748	0.5	2370	188	2108	166	2604	17	11.1		
*49	498803	hom core	315513	669	558	159480	1.08	10.3157	4.5	0.4274	4.5	1.00	0.1750	0.4	2464	221	2294	205	2606	12	6.9		
*50	498803	hom core	502778	1076	696	44282	0.81	10.5916	3.7	0.4379	3.7	0.99	0.1754	0.4	2488	185	2341	174	2610	13	5.9		
*47	498803	hom core	567112	1212	700	18775	0.44	9.7754	4.2	0.4030	4.2	0.99	0.1759	0.5	2414	204	2183	184	2615	15	9.6		
75	498803	hom core	475573	1014	566	28687	0.66	8.6447	3.7	0.3547	3.5	0.95	0.1767	1.1	2301	169	1957	137	2623	37	15.0		
*54	498803	hom core	422759	861	695	1808	1.23	14.3696	4.2	0.5888	4.1	1.00	0.1770	0.3	2774	231	2984	248	2625	11	-7.6		
64	498803	hom core	662875	1488	685	25389	0.53	8.3580	6.1	0.2906	4.8	0.78	0.2086	3.8	2271	277	1644	157	2895	124	27.6		
41	498803	hom core	705507	1539	713	204bdl	0.65	10.9158	4.3	0.3149	3.7	0.86	0.2514	2.2	2516	217	1765	131	3194	68	29.9		
228	498864	osc core	88185	147	76	49529	0.23	12.2180	3.5	0.4788	3.4	0.99	0.1851	0.4	2621	182	2522	174	2699	14	3.8		

Analysis	sample	morphology	zircon		$^{207}\text{Pb}$	U	Pb	$^{206}\text{Pb}$	Th	$^{207}\text{Pb}$	1 $\sigma$	$^{206}\text{Pb}^e$	1 $\sigma$	rho	$^{207}\text{Pb}$	1 $\sigma$	$^{207}\text{Pb}$	2 $\sigma$	$^{206}\text{Pb}$	2 $\sigma$	$^{207}\text{Pb}$	2 $\sigma$	Disc.
			(cps)	(ppm)	(ppm)	$^{204}\text{Pb}$	U	$^{235}\text{U}$	%	$^{238}\text{U}$	%	$^{206}\text{Pb}$	%	$^{235}\text{U}$	(Ma)	$^{238}\text{U}$	(Ma)	$^{206}\text{Pb}$	(Ma)				
250	498864	osc core	141875	231	121	27237	0.09	12.8314	3.3	0.4945	3.3	1.00	0.1882	0.3	2667	178	2590	172	2726	9	2.9		
243	498864	osc core	51792	64	45	8733	0.10	17.3289	3.5	0.6671	3.4	0.99	0.1884	0.5	2953	205	3295	226	2728	17	-11.6		
255	498864	osc core	12220	15	11	1544	0.27	17.5074	3.8	0.6632	3.6	0.95	0.1914	1.2	2963	224	3280	236	2755	38	-10.7		
231	498864	osc core	56824	72	49	4799	0.24	15.8594	3.5	0.5962	3.4	0.99	0.1929	0.4	2868	199	3015	208	2767	13	-5.1		
249	498864	hom rim	154534	228	127	204bdl	0.10	14.0638	3.4	0.5188	3.3	1.00	0.1966	0.3	2754	185	2694	180	2798	11	2.2		
247	498864	osc core	151805	252	140	11879	0.34	12.8388	3.3	0.4728	3.3	0.99	0.1969	0.4	2668	178	2496	166	2801	13	6.5		
246	498864	osc core	75052	97	61	14072	0.15	15.7509	3.5	0.5797	3.4	0.98	0.1971	0.7	2862	198	2948	199	2802	23	-3.0		
248	498864	osc core	50069	72	44	173801	0.42	14.7327	3.4	0.5294	3.4	0.99	0.2018	0.5	2798	191	2739	185	2841	17	2.1		
230	498864	osc core	27499	31	26	5330	0.61	19.6432	3.4	0.7021	3.3	0.99	0.2029	0.6	3074	208	3429	228	2850	19	-11.5		
229	498864	osc core	16168	19	13	1354	0.26	18.4520	3.9	0.6564	3.5	0.89	0.2039	1.8	3014	236	3253	227	2857	57	-8.0		
233	498864	osc core	27405	31	24	6824	0.29	19.3945	3.4	0.6891	3.3	0.99	0.2041	0.5	3062	206	3379	225	2860	17	-10.4		
244	498864	osc core	47784	52	38	1345	0.13	18.4027	3.5	0.6533	3.4	0.98	0.2043	0.8	3011	208	3241	219	2861	25	-7.6		
223	498864	osc core	70732	102	57	8659	0.17	14.1727	3.5	0.5027	3.4	0.99	0.2045	0.4	2761	191	2625	180	2862	14	4.9		
257	498864	osc core	66277	77	48	13692	0.11	16.5332	3.4	0.5851	3.4	0.99	0.2050	0.6	2908	200	2969	201	2866	19	-2.1		
254	498864	osc core	37065	46	29	1060	0.32	15.3835	3.5	0.5380	3.4	0.98	0.2074	0.8	2839	198	2775	189	2885	25	2.3		
222	498864	osc core	101929	143	79	4818	0.19	14.4170	3.5	0.4998	3.4	0.99	0.2092	0.5	2778	193	2613	180	2899	17	5.9		
245	498864	osc core	66912	76	53	5234	0.10	18.7093	3.4	0.6479	3.4	0.98	0.2094	0.6	3027	207	3220	217	2901	20	-6.4		
241	498864	osc core	62508	81	49	12497	0.36	15.2989	3.5	0.5294	3.5	0.98	0.2096	0.8	2834	201	2739	189	2903	25	3.4		
234	498864	osc core	109208	145	87	33383	0.36	14.8742	4.0	0.5108	4.0	0.99	0.2112	0.5	2807	224	2660	211	2915	17	5.2		
242	498864	osc core	104144	148	94	30818	0.57	14.9664	3.5	0.5122	3.4	0.99	0.2119	0.6	2813	195	2666	182	2920	18	5.2		
260	498864	osc core	43759	58	37	7989	0.41	15.7279	3.5	0.5376	3.5	0.98	0.2122	0.7	2860	202	2774	192	2922	21	3.0		
235	498864	osc core	64784	71	57	27203	0.47	20.2173	3.4	0.6904	3.3	0.99	0.2124	0.5	3102	209	3384	226	2924	17	-9.1		
256	498864	osc core	78407	104	58	11093	0.31	14.0925	4.4	0.4800	4.3	0.99	0.2130	0.5	2756	241	2527	219	2928	16	8.3		
232	498864	osc core	102898	138	88	22280	0.32	16.4329	3.4	0.5555	3.4	0.99	0.2145	0.3	2902	196	2848	192	2940	11	1.9		
237	498864	hom rim	321263	448	266	29262	0.22	15.6797	3.4	0.5286	3.3	1.00	0.2151	0.3	2857	192	2736	183	2945	9	4.3		

Analysis	sample	zircon morphology	$^{207}\text{Pb}$		U	Pb	$^{206}\text{Pb}$	Th	$^{207}\text{Pb}$	1 σ	$^{206}\text{Pb}^e$	1 σ	rho	$^{207}\text{Pb}$	1 σ	$^{207}\text{Pb}$	2 σ	$^{206}\text{Pb}$	2 σ	$^{207}\text{Pb}$	2 σ	Disc.
			(cps)	(ppm)	(ppm)		$^{204}\text{Pb}$	U	$^{235}\text{U}$	%	$^{238}\text{U}$	%		$^{206}\text{Pb}$	%	$^{235}\text{U}$	(Ma)	$^{238}\text{U}$	(Ma)	$^{206}\text{Pb}$	(Ma)	
258	498864	osc core	39440	53	35	11352	0.60	15.4280	3.4	0.5194	3.4	0.99	0.2155	0.5	2842	194	2696	182	2947	15	5.1	
224	498864	osc core	43078	58	37	204bdl	0.50	15.6912	3.3	0.5254	3.3	0.99	0.2166	0.5	2858	191	2722	180	2956	16	4.8	
236	498864	sec core	141548	225	155	56176	0.19	19.0385	3.4	0.6313	3.4	0.99	0.2187	0.4	3044	209	3155	215	2971	14	-3.7	
259	498864	osc core	68495	90	60	73172	0.55	16.2074	3.4	0.5364	3.4	0.99	0.2191	0.4	2889	195	2768	186	2974	13	4.2	
112	498877	osc core	65136	119	53	4180	0.09	10.8245	3.4	0.4311	3.4	0.99	0.1821	0.4	2508	170	2310	155	2672	14	7.9	
126	498877	osc core	154221	265	135	38292	0.07	12.4585	3.4	0.4927	3.3	0.99	0.1834	0.5	2640	178	2582	172	2684	17	2.2	
139	498877	osc core	18859	30	17	1720	0.07	13.4379	3.6	0.5292	3.5	0.98	0.1842	0.7	2711	193	2738	191	2691	23	-1.0	
142	498877	osc core	24522	37	20	1988	0.13	13.4877	3.6	0.5289	3.6	0.99	0.1850	0.6	2714	196	2737	195	2698	20	-0.8	
119	498877	osc core	31598	57	27	1895	0.09	11.4098	3.4	0.4460	3.4	0.99	0.1855	0.6	2557	174	2378	160	2703	19	7.0	
132	498877	osc core	58208	104	46	2593	0.12	10.7574	3.5	0.4203	3.4	0.99	0.1856	0.6	2502	174	2262	155	2704	18	9.6	
116	498877	osc core	37053	55	30	5309	0.09	13.5975	3.5	0.5303	3.5	0.97	0.1860	0.8	2722	193	2743	189	2707	27	-0.8	
107	498877	osc core	96340	160	87	6534	0.07	13.4202	3.4	0.5221	3.3	0.99	0.1864	0.6	2710	183	2708	180	2711	19	0.1	
131	498877	hom rim	16676	28	15	1178	0.11	13.0116	7.2	0.5061	7.1	0.99	0.1865	0.8	2680	384	2640	376	2711	28	1.5	
128	498877	osc core	105545	165	85	4204	0.06	12.6464	3.5	0.4893	3.4	0.99	0.1875	0.5	2654	184	2568	176	2720	16	3.2	
106	498877	osc core	126632	267	108	2358	0.11	9.8557	3.4	0.3813	3.4	1.00	0.1875	0.3	2421	165	2082	141	2720	9	14.0	
129	498877	osc core	31759	59	27	1267	0.17	11.0219	3.6	0.4260	3.5	0.96	0.1876	1.0	2525	182	2288	159	2722	32	9.4	
117	498877	osc core	86599	131	70	3102	0.11	13.0203	3.4	0.5028	3.3	0.98	0.1878	0.6	2681	183	2626	176	2723	20	2.1	
111	498877	osc core	52585	82	42	2971	0.06	12.7027	4.0	0.4878	3.7	0.95	0.1889	1.3	2658	210	2561	192	2732	41	3.6	
114	498877	osc core	46876	86	43	2690	0.16	12.2813	4.4	0.4708	4.3	0.98	0.1892	0.8	2626	229	2487	213	2735	25	5.3	
118	498877	osc core	36665	57	31	1454	0.13	13.3327	3.5	0.5109	3.4	0.98	0.1893	0.7	2704	189	2661	183	2736	22	1.6	
141	498877	osc core	64611	102	54	3773	0.11	12.9884	3.4	0.4963	3.3	0.99	0.1898	0.5	2679	181	2598	174	2740	15	3.0	
113	498877	osc rim	486282	778	375	3853	0.10	11.9575	4.0	0.4546	3.9	0.98	0.1908	0.8	2601	206	2416	187	2749	27	7.1	
143	498877	osc core	25226	42	21	1034	0.11	12.6365	3.6	0.4767	3.5	0.97	0.1923	0.9	2653	190	2513	175	2762	29	5.3	
120	498877	osc core	110110	237	107	1049	0.12	11.3658	3.9	0.4249	3.7	0.96	0.1940	1.1	2554	198	2283	169	2776	37	10.6	
140	498877	sec core	90104	135	78	12090	0.15	14.4513	3.5	0.5393	3.3	0.96	0.1944	1.0	2780	193	2780	185	2779	32	0.0	

Analysis	sample	zircon morphology	<sup>207</sup> Pb			U	Pb	<sup>206</sup> Pb	Th	<sup>207</sup> Pb	1 σ	<sup>206</sup> Pb <sup>e</sup>	1 σ	rho	<sup>207</sup> Pb	1 σ	<sup>207</sup> Pb	2 σ	<sup>206</sup> Pb	2 σ	<sup>207</sup> Pb	2 σ	Disc.
			(cps)	(ppm)	(ppm)	<sup>204</sup> Pb	U	<sup>235</sup> U	%	<sup>238</sup> U	%	<sup>206</sup> Pb	%	<sup>235</sup> U	(Ma)	<sup>238</sup> U	(Ma)	<sup>206</sup> Pb	(Ma)	<sup>206</sup> Pb	(Ma)		
125	498877	osc rim	39938	60	32	2076	0.13	13.3684	3.6	0.4988	3.5	0.96	0.1944	1.0	2706	194	2609	180	2780	33	3.6		
127	498877	osc core	26638	41	24	343	0.29	14.0643	3.6	0.5231	3.5	0.98	0.1950	0.8	2754	197	2713	190	2785	26	1.5		
137	498877	osc core	45350	75	40	1517	0.13	13.5312	3.5	0.5010	3.4	0.97	0.1959	0.9	2717	190	2618	177	2792	29	3.7		
133	498877	sec core	50766	79	46	2151	0.20	14.5582	3.5	0.5368	3.4	0.99	0.1967	0.6	2787	193	2770	189	2799	19	0.6		
130	498877	osc core	140351	203	115	5993	0.05	14.8882	3.6	0.5400	3.4	0.94	0.1999	1.3	2808	204	2784	190	2826	41	0.9		
124	498877	hi U osc core	729987	1075	637	90179	0.21	15.3024	3.5	0.5485	3.4	0.96	0.2024	0.9	2834	199	2819	191	2845	31	0.5		
115	498877	hi U osc core	277365	446	222	1942	0.16	13.0655	3.6	0.4556	3.5	0.99	0.2080	0.6	2684	193	2420	171	2890	19	9.8		
204	498892	hom core	56022	84	42	15103	0.03	14.2535	3.3	0.4717	3.2	0.98	0.2191	0.7	2767	182	2491	160	2974	21	10.0		
203	498892	hom core	123891	183	113	448595	0.44	16.0770	3.2	0.5145	3.2	0.99	0.2266	0.4	2881	184	2676	170	3029	13	7.1		
185	498892	pat core	110335	160	88	41636	0.11	15.7578	3.3	0.5038	3.2	0.99	0.2268	0.4	2862	187	2630	170	3030	13	8.1		
205	498892	pat rim	47408	69	43	39939	0.50	16.1099	3.3	0.5134	3.2	0.99	0.2276	0.5	2883	188	2671	172	3035	15	7.4		
192	498892	pat core	72286	107	64	80438	0.47	15.1803	3.4	0.4827	3.3	0.97	0.2281	0.8	2827	189	2539	166	3039	25	10.2		
184	498892	hom rim	120410	172	104	33711	0.31	16.8296	3.3	0.5261	3.2	0.99	0.2320	0.5	2925	190	2725	175	3066	18	6.8		
182	498892	hom rim	55845	86	43	4072	0.62	12.9121	4.7	0.4034	4.7	0.99	0.2322	0.7	2673	252	2184	204	3067	21	18.3		
183	498892	pat core	230768	293	194	44238	0.50	18.2537	3.4	0.5208	3.4	0.98	0.2542	0.7	3003	206	2703	181	3211	23	10.0		
195	498892	hom rim	211150	271	187	10605	0.58	20.1394	3.6	0.5685	3.6	0.99	0.2569	0.5	3098	225	2902	209	3228	16	6.3		
209	498892	hom core	355899	440	277	119901	0.18	19.5779	3.5	0.5481	3.4	0.99	0.2591	0.4	3071	213	2817	194	3241	11	8.3		
180	498892	hom core	367828	437	264	18139	0.28	18.5233	3.4	0.5013	3.4	0.99	0.2680	0.5	3017	205	2619	176	3294	15	13.2		
190	498892	hom core	225322	250	183	62970	0.57	21.0724	3.5	0.5681	3.4	0.99	0.2690	0.4	3142	218	2900	200	3300	13	7.7		
208	498892	pat core	567440	640	569	486893	0.46	21.0025	3.3	0.5520	3.3	0.99	0.2760	0.4	3139	207	2833	186	3340	12	9.7		
206	498892	hom core	199198	222	158	204bdl	0.43	21.9252	3.3	0.5744	3.3	0.99	0.2769	0.6	3180	211	2926	191	3345	18	8.0		
197	498892	hom core	569852	657	552	80864	0.48	20.9390	3.3	0.5479	3.2	0.97	0.2772	0.8	3136	209	2816	183	3347	23	10.2		
196	498892	osc rim	130292	163	102	25868	0.56	17.8407	3.8	0.4657	3.8	1.00	0.2778	0.3	2981	227	2465	187	3351	11	17.3		
202	498892	pat rim	244528	269	224	45615	1.13	22.4491	3.2	0.5857	3.2	0.99	0.2780	0.3	3203	204	2972	188	3352	10	7.2		
191	498892	hom core	180635	223	172	204bdl	0.44	24.6790	3.4	0.6396	3.3	0.97	0.2799	0.8	3296	224	3187	209	3362	26	3.3		

Analysis	sample	morphology	zircon		$^{207}\text{Pb}$	U	Pb	$^{206}\text{Pb}$	Th	$^{207}\text{Pb}$	1 $\sigma$	$^{206}\text{Pb}^e$	1 $\sigma$	rho	$^{207}\text{Pb}$	1 $\sigma$	$^{207}\text{Pb}$	2 $\sigma$	$^{206}\text{Pb}$	2 $\sigma$	$^{207}\text{Pb}$	2 $\sigma$	Disc.
			(cps)	(ppm)	(ppm)	$^{204}\text{Pb}$	U	$^{235}\text{U}$	%	$^{238}\text{U}$	%	$^{206}\text{Pb}$	%	$^{235}\text{U}$	(Ma)	$^{238}\text{U}$	(Ma)	$^{206}\text{Pb}$	(Ma)				
198	498892	hom core	172253	174	136	132184	0.72	22.4898	3.3	0.5745	3.3	0.99	0.2839	0.4	3205	214	2926	194	3385	12	8.7		
179	498892	hom core	276527	273	328	89268	2.84	25.6508	3.5	0.6452	3.4	0.98	0.2883	0.6	3333	232	3210	219	3409	20	3.7		
193	498892	hom core	792246	730	642	249960	0.61	28.2393	3.6	0.6964	3.5	0.97	0.2941	0.9	3427	249	3407	240	3439	28	0.6		
207	498892	hom core	441248	429	411	87373	1.42	24.7996	3.2	0.6113	3.2	1.00	0.2942	0.3	3300	214	3075	198	3440	8	6.8		
189	498892	hom core	809339	768	906	162740	0.44	26.3936	3.6	0.5913	3.3	0.93	0.3237	1.3	3361	239	2995	199	3588	39	10.9		
210	498921	hom rim	547040	620	511	109960	0.94	21.7789	3.4	0.6022	3.3	0.99	0.2623	0.5	3174	214	3039	202	3261	17	4.3		
216	498921	hom rim	245997	273	191	204bdl	0.33	21.4327	3.3	0.5823	3.3	0.99	0.2669	0.5	3158	209	2958	193	3288	15	6.3		
247	498921	hom core	384100	443	333	204bdl	0.61	21.7112	3.2	0.5852	3.2	1.00	0.2691	0.3	3171	202	2970	189	3301	8	6.3		
229	498921	pat core	353725	425	306	112031	0.51	21.4869	3.4	0.5765	3.3	0.99	0.2703	0.5	3161	212	2935	195	3308	15	7.2		
218	498921	osc core	626962	69	43	204bdl	0.02	21.0800	3.3	0.5653	3.3	0.99	0.2705	0.5	3142	209	2888	190	3309	16	8.1		
224	498921	hom core	370087	415	330	81249	0.86	22.2499	3.2	0.5956	3.2	0.99	0.2709	0.4	3195	204	3012	191	3311	12	5.7		
232	498921	hom rim	197647	234	198	39258	1.21	22.3989	3.4	0.5966	3.4	0.99	0.2723	0.5	3201	219	3016	204	3319	14	5.8		
234	498921	hom core	123061	132	94	221119	0.23	23.0071	3.3	0.6121	3.3	0.99	0.2726	0.5	3227	213	3078	201	3321	14	4.6		
221	498921	pat core	462610	523	420	204bdl	0.89	22.6229	3.2	0.6017	3.2	1.00	0.2727	0.3	3211	206	3037	194	3322	9	5.4		
248	498921	pat core	437395	496	378	204bdl	0.69	21.7459	3.2	0.5763	3.2	1.00	0.2737	0.3	3172	202	2933	186	3327	8	7.5		
236	498921	osc core	315445	349	270	210401	0.71	22.1918	3.2	0.5873	3.2	1.00	0.2740	0.3	3192	203	2979	189	3329	8	6.7		
215	498921	hom core	434385	460	367	204bdl	0.77	22.2347	3.2	0.5881	3.2	1.00	0.2742	0.3	3194	204	2982	190	3330	9	6.7		
235	498921	pat core	127114	132	101	58972	0.33	24.3205	4.0	0.6406	3.9	0.99	0.2754	0.6	3281	260	3191	250	3337	19	2.7		
217	498921	hom rim	251371	251	202	204bdl	0.65	23.0305	3.3	0.6060	3.3	0.99	0.2756	0.4	3228	215	3054	202	3338	12	5.4		
228	498921	pat core	250936	263	197	204bdl	0.52	22.8436	3.3	0.6004	3.3	0.99	0.2760	0.4	3220	212	3031	198	3340	13	5.9		
233	498921	pat rim	272966	361	214	15113	0.11	19.8378	4.4	0.5209	4.4	1.00	0.2762	0.4	3083	272	2703	237	3342	13	12.3		
223	498921	hom core	100650	108	71	204bdl	0.06	22.0449	3.2	0.5786	3.2	0.99	0.2763	0.4	3186	205	2943	188	3342	12	7.6		
230	498921	hom core	106724	111	89	5430	0.26	24.8804	3.2	0.6528	3.2	0.99	0.2764	0.4	3304	212	3239	206	3343	13	1.9		
241	498921	hom core	279613	316	242	26696	0.72	22.2675	3.3	0.5830	3.3	1.00	0.2770	0.3	3195	214	2961	197	3346	10	7.3		
242	498921	osc core	193639	204	154	103527	0.50	22.8306	3.2	0.5972	3.2	1.00	0.2773	0.3	3220	207	3019	193	3348	10	6.2		

Analysis	sample	morphology	zircon		<sup>207</sup> Pb	U	Pb	<sup>206</sup> Pb	Th	<sup>207</sup> Pb	1 σ	<sup>206</sup> Pb <sup>e</sup>	1 σ	rho	<sup>207</sup> Pb	1 σ	<sup>207</sup> Pb	2 σ	<sup>206</sup> Pb	2 σ	<sup>207</sup> Pb	2 σ	Disc.
			(cps)	(ppm)	(ppm)	<sup>204</sup> Pb	U	<sup>235</sup> U	%	<sup>238</sup> U	%	<sup>206</sup> Pb	%	<sup>235</sup> U	(Ma)	<sup>238</sup> U	(Ma)	<sup>206</sup> Pb	(Ma)	<sup>207</sup> Pb	(Ma)		
219	498921	osc core	175635	188	136	204bdl	0.41	22.4587	3.2	0.5866	3.2	0.99	0.2777	0.3	3204	206	2976	190	3350	11	7.1		
220	498921	osc core	304696	345	254	204bdl	0.54	22.3262	3.3	0.5831	3.3	0.99	0.2777	0.4	3198	210	2961	194	3350	11	7.4		
211	498921	osc core	38938	42	31	41710	0.38	23.9852	3.3	0.6252	3.3	0.97	0.2782	0.8	3268	219	3131	204	3353	24	4.2		
244	498921	hom core	198380	223	173	123591	0.76	22.2627	3.3	0.5795	3.3	1.00	0.2786	0.3	3195	210	2947	193	3355	9	7.8		
222	498921	osc core	172059	182	137	45603	0.59	22.1710	3.4	0.5766	3.3	0.99	0.2789	0.4	3191	215	2935	197	3357	11	8.0		
246	498921	hom rim	179197	197	160	204bdl	0.89	23.6565	3.2	0.6149	3.2	1.00	0.2790	0.3	3254	208	3090	196	3357	10	5.1		
243	498921	hom rim	87469	91	65	34150	0.53	21.9773	3.3	0.5708	3.3	0.99	0.2793	0.4	3183	211	2911	191	3359	13	8.5		
231	498921	osc rim	248899	258	190	204bdl	0.49	22.1071	3.4	0.5741	3.4	1.00	0.2793	0.3	3188	217	2924	199	3359	9	8.3		
245	498921	osc core	87852	92	67	20557	0.37	23.0944	3.2	0.5955	3.2	0.99	0.2813	0.3	3231	206	3012	191	3370	10	6.8		
237	498921	osc core	59529	60	45	9648	0.45	22.9611	3.7	0.5911	3.6	0.99	0.2817	0.5	3225	236	2994	217	3373	16	7.2		
29	498937	pat rim	53283	46	38	3623	0.31	30.1730	3.3	0.6514	3.2	0.97	0.3359	0.9	3492	234	3234	209	3644	26	7.4		
38	498937	pat core	60495	42	38	7470	0.64	32.3230	3.2	0.6616	3.2	0.99	0.3543	0.5	3560	231	3273	209	3726	17	8.1		
9	498937	osc core	111660	74	72	23288	0.70	34.9812	3.2	0.7039	3.2	0.98	0.3604	0.6	3638	235	3435	217	3752	19	5.6		
13	498937	pat core	85000	57	53	14602	0.67	33.8352	3.3	0.6725	3.3	0.98	0.3649	0.6	3605	239	3316	216	3770	19	8.0		
34	498937	osc core	107143	69	64	12979	0.64	34.1451	3.2	0.6746	3.2	0.99	0.3671	0.4	3614	232	3324	212	3779	11	8.0		
28	498937	pat rim	114299	78	68	3316	0.29	34.7404	3.3	0.6839	3.2	0.99	0.3684	0.5	3631	236	3359	216	3785	15	7.5		
23	498937	pat core	1209905	900	593	45209	0.03	28.0521	3.8	0.5493	3.3	0.87	0.3704	1.9	3421	257	2822	184	3793	57	17.5		
11	498937	pat core	66830	45	37	1425	0.36	29.7892	3.3	0.5828	3.2	0.97	0.3707	0.7	3480	231	2960	191	3794	23	14.9		
42	498937	hom core	87452	55	54	204bdl	0.92	34.8083	3.3	0.6771	3.2	0.99	0.3728	0.5	3633	236	3333	215	3803	14	8.3		
*15	498937	hom core	74272	48	43	204bdl	0.49	33.7646	3.5	0.6554	3.3	0.95	0.3736	1.1	3603	252	3249	216	3806	32	9.8		
*26	498937	osc rim	59432	36	34	204bdl	0.55	35.8222	3.2	0.6930	3.2	0.98	0.3749	0.6	3662	238	3394	217	3811	18	7.3		
*35	498937	osc core	117742	72	75	7442	0.97	36.9923	3.3	0.7128	3.3	0.99	0.3764	0.3	3693	243	3469	227	3817	10	6.1		
*40	498937	osc core	57621	36	36	42277	0.72	38.3616	3.2	0.7364	3.2	0.99	0.3778	0.4	3729	240	3557	227	3823	13	4.6		
*33	498937	osc core	73211	43	45	15533	0.66	40.1274	3.2	0.7667	3.2	0.99	0.3796	0.5	3774	243	3669	233	3830	15	2.8		
*24	498937	hom core	127879	78	81	5222	0.82	37.4359	3.2	0.7132	3.2	0.99	0.3807	0.4	3705	239	3471	222	3834	12	6.3		

Analysis	sample	morphology	zircon		$^{207}\text{Pb}$	U	Pb	$^{206}\text{Pb}$	Th	$^{207}\text{Pb}$	1 $\sigma$	$^{206}\text{Pb}^e$	1 $\sigma$	rho	$^{207}\text{Pb}$	1 $\sigma$	$^{207}\text{Pb}$	2 $\sigma$	$^{206}\text{Pb}$	2 $\sigma$	$^{207}\text{Pb}$	2 $\sigma$	Disc.
			(cps)	(ppm)	(ppm)	$^{204}\text{Pb}$	U	$^{235}\text{U}$	%	$^{238}\text{U}$	%	$^{206}\text{Pb}$	%	$^{235}\text{U}$	(Ma)	$^{238}\text{U}$	(Ma)	$^{206}\text{Pb}$	(Ma)				
7*	498937	osc core	199079	131	125	26008	0.66	36.2429	3.3	0.6881	3.3	0.99	0.3820	0.4	3673	242	3375	220	3840	13	8.1		
3*6	498937	hom rim	93554	56	52	1600	0.49	35.3191	3.5	0.6680	3.4	0.97	0.3835	0.9	3648	257	3298	225	3845	26	9.6		
*8	498937	osc core	75911	48	43	16683	0.42	37.1840	3.4	0.6999	3.2	0.95	0.3853	1.1	3698	252	3420	221	3853	32	7.5		
*21	498937	osc rim	112294	77	79	5954	0.29	44.0286	3.3	0.8141	3.2	0.98	0.3922	0.7	3866	256	3840	248	3880	22	0.7		
14	498937	osc core	170893	109	92	9529	0.33	34.5914	3.4	0.6373	3.2	0.95	0.3937	1.0	3627	244	3178	203	3885	32	12.4		
39	498937	osc core	71825	37	29	6131	0.37	32.3874	3.9	0.5966	3.5	0.90	0.3937	1.7	3562	279	3016	214	3885	51	15.3		
*25	498937	osc core	323059	186	166	8304	0.15	38.7446	3.2	0.7117	3.2	0.98	0.3948	0.6	3739	243	3465	220	3889	19	7.3		
*37	498937	hom core	325648	181	172	57609	0.56	39.7153	3.4	0.6976	3.4	0.98	0.4129	0.7	3764	258	3412	229	3957	22	9.4		
10	498937	osc core	373971	218	208	21304	0.74	36.7653	3.3	0.6400	3.3	0.99	0.4167	0.4	3687	242	3189	208	3970	11	13.5		
27	498937	osc core	713654	387	408	41329	0.71	42.5764	3.2	0.7404	3.2	1.00	0.4170	0.3	3833	244	3572	227	3972	9	6.8		
41	498937	hom core	75704	42	48	20601	0.65	48.4235	3.3	0.8341	3.2	0.97	0.4211	0.8	3960	260	3910	248	3986	24	1.3		
20	498937	osc core	179718	94	94	204bdl	0.37	43.5324	3.2	0.7469	3.2	0.99	0.4227	0.3	3855	247	3596	229	3992	10	6.7		
22	498937	osc core	79643	38	44	4771	0.53	49.3356	3.2	0.8413	3.2	0.99	0.4253	0.4	3979	254	3935	249	4001	13	1.1		
16	498937	osc core	239908	127	124	12089	0.56	40.4669	3.3	0.6822	3.2	0.99	0.4302	0.4	3782	247	3353	218	4018	11	11.4		
*143	498945	hom rim	73724	98	58	204bdl	0.04	17.4348	3.2	0.5505	3.2	0.99	0.2297	0.4	2959	190	2827	180	3050	13	4.5		
*137	498945	hom rim	96019	132	75	204bdl	0.02	16.7747	3.2	0.5296	3.2	0.99	0.2297	0.3	2922	186	2740	173	3050	11	6.2		
*119	498945	hom rim	85119	114	69	48346	0.02	17.8467	3.2	0.5620	3.2	0.99	0.2303	0.5	2982	192	2875	183	3054	15	3.6		
*177	498945	hom rim	84594	118	66	204bdl	0.01	16.7834	3.2	0.5262	3.2	0.99	0.2313	0.3	2923	188	2726	174	3061	10	6.7		
140	498945	hom rim	82172	110	52	204bdl	0.02	13.9269	4.4	0.4365	4.4	0.99	0.2314	0.5	2745	242	2335	204	3062	15	14.9		
*167	498945	hom rim	64780	88	51	17275	0.03	17.2520	3.2	0.5399	3.2	0.99	0.2318	0.4	2949	189	2783	177	3064	13	5.6		
178	498945	hom core	39636	47	27	204bdl	0.15	16.7489	3.3	0.5144	3.2	0.96	0.2361	0.9	2921	193	2675	170	3094	29	8.4		
138	498945	hom core	44318	54	36	204bdl	0.25	19.0665	3.2	0.5815	3.2	0.99	0.2378	0.5	3045	197	2955	189	3105	15	3.0		
126	498945	hom core	48390	61	38	21048	0.23	18.1017	3.4	0.5331	3.2	0.94	0.2463	1.1	2995	205	2754	178	3161	36	8.0		
157	498945	hom core	51647	58	41	18510	0.30	21.1146	3.2	0.6167	3.2	0.99	0.2483	0.5	3144	203	3097	198	3174	16	1.5		
141	498945	hom core	69864	88	56	204bdl	0.21	19.3473	3.5	0.5501	3.3	0.93	0.2551	1.2	3059	213	2826	184	3217	39	7.6		

Analysis	sample	zircon morphology	$^{207}\text{Pb}$		U	Pb	$^{206}\text{Pb}$	Th	$^{207}\text{Pb}$	1 $\sigma$	$^{206}\text{Pb}^e$	1 $\sigma$	rho	$^{207}\text{Pb}$	1 $\sigma$	$^{207}\text{Pb}$	2 $\sigma$	$^{206}\text{Pb}$	2 $\sigma$	$^{207}\text{Pb}$	2 $\sigma$	Disc.
			(cps)	(ppm)	(ppm)		$^{204}\text{Pb}$	U	$^{235}\text{U}$	%	$^{238}\text{U}$	%		$^{206}\text{Pb}$	%	$^{235}\text{U}$	(Ma)	$^{238}\text{U}$	(Ma)	$^{206}\text{Pb}$	(Ma)	
176	498945	hom core	42003	49	35	204bdl	0.31	21.7134	3.4	0.6108	3.3	0.97	0.2578	0.8	3171	216	3073	203	3234	27	3.1	
132	498945	hom core	36293	44	27	4891	0.34	18.3117	3.5	0.5079	3.4	0.98	0.2615	0.7	3006	211	2648	182	3256	21	11.9	
144	498945	hom core	37827	42	32	4430	0.43	23.5047	3.5	0.6461	3.4	0.97	0.2638	0.8	3248	228	3213	220	3270	25	1.1	
153	498945	pat core	21735	23	17	204bdl	0.46	22.3562	3.5	0.6130	3.2	0.93	0.2645	1.3	3199	224	3082	200	3274	41	3.7	
139	498945	hom core	25039	27	19	204bdl	0.43	20.7803	3.4	0.5650	3.3	0.98	0.2667	0.7	3128	211	2887	191	3287	21	7.7	
166	498945	hom core	27114	29	21	204bdl	0.39	21.5744	5.3	0.5859	5.2	0.99	0.2671	0.6	3165	333	2973	311	3289	19	6.1	
152	498945	osc core	32593	33	24	204bdl	0.32	22.6179	3.8	0.6096	3.6	0.97	0.2691	1.0	3211	241	3068	223	3301	30	4.4	
165	498945	pat core	38150	41	28	8918	0.36	21.2030	3.4	0.5677	3.3	0.96	0.2709	0.9	3148	216	2898	191	3311	29	7.9	
156	498945	pat core	37813	41	32	204bdl	0.59	23.8169	3.4	0.6361	3.3	0.97	0.2716	0.8	3261	219	3174	207	3315	24	2.7	
154	498945	pat core	55138	68	50	204bdl	0.40	23.1049	3.2	0.6143	3.2	0.99	0.2728	0.5	3231	209	3087	197	3322	16	4.5	
151	498945	hom core	86421	93	69	21885	0.63	21.7263	3.3	0.5776	3.2	0.98	0.2728	0.6	3172	208	2939	189	3322	19	7.3	
146	498945	hom core	23436	23	18	204bdl	0.43	23.9297	3.3	0.6289	3.2	0.97	0.2760	0.8	3266	217	3145	203	3340	24	3.7	
172	498945	pat core	28553	28	24	5996	0.56	25.9603	3.3	0.6760	3.2	0.98	0.2785	0.6	3345	220	3329	215	3355	20	0.5	
142	498945	hom core	38729	38	32	6787	0.97	23.3741	3.3	0.6054	3.2	0.98	0.2800	0.6	3243	211	3052	195	3363	19	5.9	
117	498945	hom core	25911	23	22	5156	0.61	29.2218	3.3	0.7560	3.3	0.98	0.2803	0.6	3461	231	3630	238	3365	20	-4.9	
145	498945	hom core	77502	110	135	109640	2.37	28.5670	3.3	0.7372	3.2	0.98	0.2811	0.6	3439	227	3560	231	3369	19	-3.5	
129	498945	hom core	18581	18	14	204bdl	0.52	23.7093	3.5	0.6115	3.4	0.97	0.2812	0.9	3257	226	3076	206	3370	28	5.5	
127	498945	hom core	20582	20	15	204bdl	0.51	23.6855	3.3	0.6087	3.2	0.98	0.2822	0.6	3256	213	3065	197	3375	20	5.9	
150	498945	hom core	37760	36	32	6906	1.06	25.5815	3.2	0.6566	3.2	0.99	0.2826	0.5	3331	215	3254	207	3377	15	2.3	
130	498945	hom core	22468	21	17	204bdl	0.59	24.0453	3.3	0.6152	3.2	0.98	0.2835	0.6	3270	215	3091	199	3382	19	5.5	
133	498945	hom core	46574	45	37	204bdl	0.91	22.9227	3.2	0.5863	3.2	0.99	0.2835	0.5	3224	209	2975	190	3383	16	7.7	
159	498945	hom core	28876	28	21	204bdl	0.61	23.0206	3.2	0.5864	3.2	0.98	0.2847	0.6	3228	209	2975	189	3389	19	7.8	
169	498945	hom core	25965	26	21	34323	0.58	26.0669	3.3	0.6623	3.3	0.98	0.2855	0.6	3349	223	3276	214	3393	19	2.2	
168	498945	pat core	39210	42	31	11995	0.71	21.5438	3.3	0.5468	3.3	0.99	0.2857	0.5	3163	208	2812	183	3395	15	11.1	
131	498945	hom core	41727	39	35	204bdl	0.93	26.1716	3.3	0.6639	3.2	0.99	0.2859	0.6	3353	218	3282	211	3396	17	2.1	

Analysis	sample	zircon morphology	$^{207}\text{Pb}$	U	Pb	$^{206}\text{Pb}$	Th	$^{207}\text{Pb}$	1 $\sigma$	$^{206}\text{Pb}^e$	1 $\sigma$	rho	$^{207}\text{Pb}$	1 $\sigma$	$^{207}\text{Pb}$	2 $\sigma$	$^{206}\text{Pb}$	2 $\sigma$	$^{207}\text{Pb}$	2 $\sigma$	Disc.
			(cps)	(ppm)	(ppm)	$^{204}\text{Pb}$	U	$^{235}\text{U}$	%	$^{238}\text{U}$	%	$^{206}\text{Pb}$	%	$^{235}\text{U}$	(Ma)	$^{238}\text{U}$	(Ma)	$^{206}\text{Pb}$	(Ma)		
120	498945	hom core	39186	37	31	36045	0.97	23.3983	3.3	0.5924	3.2	0.98	0.2864	0.6	3244	213	2999	194	3398	19	7.5
116	498945	hom core	37527	36	29	436749	0.75	24.5102	3.2	0.6205	3.2	0.99	0.2865	0.5	3289	213	3112	199	3399	16	5.4
164	498945	hom core	23740	23	18	6306	0.57	24.2950	3.3	0.6109	3.3	0.98	0.2884	0.6	3280	218	3073	201	3409	19	6.3
118	498945	hom core	37851	37	30	4506	0.73	25.3785	3.2	0.6349	3.2	0.99	0.2899	0.5	3323	214	3169	201	3417	16	4.6
128	498945	hom core	31372	27	27	42711	0.74	32.2706	3.4	0.7988	3.3	0.98	0.2930	0.6	3559	242	3785	252	3434	20	-6.4
170	498945	pat core	32364	35	35	204bdl	0.45	35.0775	3.3	0.8469	3.2	0.97	0.3004	0.8	3641	244	3955	256	3472	26	-8.6
155	498945	pat core	29601	25	21	8432	0.85	24.3664	3.8	0.5780	3.7	0.99	0.3058	0.6	3283	247	2940	218	3500	18	10.4